NASA TECHNICAL MEMORANDUM

NASA TM - 78,443

NASA TM-78,443

CALCULATED HOVERING HELICOPTER FLIGHT DYNAMICS WITH A CIRCULATION CONTROLLED ROTOR

Wayne Johnson
Ames Research Center and
Aeromechanics Laboratory
U.S. Army Aviation R&D Command
Ames Research Center
Moffett Field, Calif. 94035

and

Inderjit Chopra
Ames Research Center
Moffett Field, Calif. 94035

September 1977

CALCULATED HOVERING HELICOPTER FLIGHT DYNAMICS WITH A CIRCULATION CONTROLLED ROTOR

Wayne Johnson

Ames Research Center, NASA
and
Aeromechanics Laboratory, U.S. Army Aviation R&D Command
Ames Research Center
Moffett Field, Calif. 94035

Inderjit Chopra

NRC Postdoctoral Research Associate
Ames Research Center, NASA

SUMMARY

The flight dynamics of a hovering helicopter with a circulation controlled rotor are analyzed. The influence of the rotor blowing coefficient on the calculated roots of the longitudinal and lateral motion is examined for a range of values of the rotor lift and the blade flap frequency. The control characteristics of a helicopter with a circulation controlled rotor are discussed. The principal effect of the blowing is a reduction in the rotor speed stability derivative. Above a critical level of blowing coefficient, which depends on the flap frequency and rotor lift, negative speed stability is produced and the dynamic characteristics of the helicopter are radically altered. The handling qualities of a helicopter with negative speed stability are probably unacceptable without a stability augmentation system.

INTRODUCTION

A circulation controlled rotor uses blowing at the blade trailing edge to control the rotor blade lift, in place of the geometric pitch control of conventional rotors. The blade section lift is given by the product

of the dynamic pressure, chord, and lift coefficient -- $L = \frac{1}{2}\rho V^2 c\, c_\ell(\alpha, C_\mu)$ -- where the lift coefficient depends now on the blowing coefficient C_μ as well as on the angle-of-attack. The blowing coefficient is defined as $C_\mu = \dot{m} V_j / (\frac{1}{2}\rho V^2 c)$, where $\dot{m}V_j$ is the jet momentum. With a conventional rotor a perturbation of the blade inplane velocity V influences the lift by changing the section dynamic pressure and angle-of-attack. With a circulation controlled rotor, inplane velocity perturbations influence the lift also by changing the section blowing coefficient:

$$\delta L = \tfrac{1}{2}\rho V^2 c \left(c_{\ell_\alpha} \delta\alpha + c_{\ell_\mu} \delta C_\mu + 2 c_\ell (\delta V/V) \right)$$

$$= \tfrac{1}{2}\rho V^2 c \left(c_{\ell_\alpha} \delta\alpha + 2(c_\ell - C_\mu c_{\ell_\mu})(\delta V/V) \right)$$

where $c_{\ell_\alpha} = \partial c_\ell / \partial \alpha$ and $c_{\ell_\mu} = \partial c_\ell / \partial C_\mu$. Assuming that the jet momentum is fixed, we have used

$$\delta C_\mu = \left(\frac{\dot{m}V_j}{\frac{1}{2}\rho c} \right) \left(-\frac{2\,\delta V}{V^3} \right) = -2 C_\mu \frac{\delta V}{V}$$

The additional lift change due to inplane velocity perturbations with trailing edge blowing will alter the dynamic characteristics of the circulation controlled rotor compared to conventional rotors. One concern is the influence of the blowing on the helicopter flight dynamics. This report presents the results of an analysis of the hovering helicopter flight dynamics with a circulation controlled rotor.

EQUATIONS OF MOTION

Consider a hovering helicopter with the center of gravity a distance h below the rotor hub, and on the shaft axis. Then the longitudinal/lateral dynamics decouple from the helicopter vertical and yaw motions. The degrees of freedom of the helicopter rigid body motion are the longitudinal velocity $\dot{x}_F$, the lateral velocity $\dot{y}_F$, the pitch angle θ_F, and the roll angle ϕ_F. For helicopter flight dynamics analyses it is generally sufficient to consider a quasistatic model for the rotor hub reactions in response to shaft motion, control, and gusts. With the quasistatic or low frequency solution, the

rotor model does not add degrees of freedom to the system, rather the rotor is represented by a set of stability derivatives. Cyclic blowing control $\Delta C_\mu = \delta_{1c}\cos\Psi + \delta_{1s}\sin\Psi$ is considered, as well as conventional cyclic pitch control $\Delta\Theta = \theta_{1c}\cos\Psi + \theta_{1s}\sin\Psi$.

Thus in Laplace form the equations of motion for helicopter longitudinal and lateral dynamics in hover are:

$$\begin{bmatrix} s - X_u & -X_v & -X_q s + g & -X_p s \\ -Y_u & s - Y_v & -Y_q s & -Y_p s - g \\ -M_u & -M_v & s^2 - M_q s & -M_p s \\ -L_u & -L_v & -L_q s & s^2 - L_p s \end{bmatrix} \begin{pmatrix} \dot{x}_F \\ \dot{y}_F \\ \theta_F \\ \phi_F \end{pmatrix}$$

$$= \begin{bmatrix} X_u & X_v & X_{\theta_s} & X_{\theta_c} & X_{\delta_s} & X_{\delta_c} \\ Y_u & Y_v & Y_{\theta_s} & Y_{\theta_c} & Y_{\delta_s} & Y_{\delta_c} \\ M_u & M_v & M_{\theta_s} & M_{\theta_c} & M_{\delta_s} & M_{\delta_c} \\ L_u & L_v & L_{\theta_s} & L_{\theta_c} & L_{\delta_s} & L_{\delta_c} \end{bmatrix} \begin{pmatrix} u_G \\ v_G \\ \theta_{1s} \\ \theta_{1c} \\ \delta_{1s} \\ \delta_{1c} \end{pmatrix}$$

(see reference 1). Here s is the Laplace variable; g is the acceleration due to gravity; and u_G and v_G are the longitudinal and lateral gust velocities. The rotor couples the helicopter longitudinal and lateral motions, but it is convenient and often sufficiently accurate to decouple the equations and analyze the longitudinal and lateral dynamics separately. The decoupled longitudinal and lateral equations of motion are:

$$\begin{bmatrix} s - X_u & -X_q s + g \\ -M_u & s^2 - M_q s \end{bmatrix} \begin{pmatrix} \dot{x}_F \\ \theta_F \end{pmatrix} = \begin{bmatrix} X_u & X_{\theta_s} & X_{\delta_s} \\ M_u & M_{\theta_s} & M_{\delta_s} \end{bmatrix} \begin{pmatrix} u_G \\ \theta_{1s} \\ \delta_{1s} \end{pmatrix}$$

$$\begin{bmatrix} s - Y_v & -Y_p s - g \\ -L_v & s^2 - L_p s \end{bmatrix} \begin{pmatrix} \dot{y}_F \\ \phi_F \end{pmatrix} = \begin{bmatrix} Y_v & Y_{\theta_c} & Y_{\delta_c} \\ L_v & L_{\theta_c} & L_{\delta_c} \end{bmatrix} \begin{pmatrix} v_G \\ \theta_{1c} \\ \delta_{1c} \end{pmatrix}$$

These equations invert to

$$\begin{pmatrix} \dot{x}_F \\ \theta_F \end{pmatrix} = \frac{1}{\Delta} \begin{pmatrix} X_{\theta_s} s^2 + (X_q M_{\theta_s} - X_{\theta_s} M_q)s - M_{\theta_s} g \\ M_{\theta_s} s + (X_{\theta_s} M_u - X_u M_{\theta_s}) \end{pmatrix} \theta_{1s}$$

$$+ \frac{1}{\Delta} \begin{pmatrix} X_{\delta_s} s^2 + (X_q M_{\delta_s} - X_{\delta_s} M_q)s - M_{\delta_s} g \\ M_{\delta_s} s + (X_{\delta_s} M_u - X_u M_{\delta_s}) \end{pmatrix} \delta_{1s}$$

$$+ \frac{1}{\Delta} \begin{pmatrix} X_u s^2 + (X_q M_u - X_u M_q)s - M_u g \\ M_u s \end{pmatrix} u_G$$

where $\Delta = s^3 - (X_u + M_q)s^2 + (X_u M_q - X_q M_u)s + g M_u$; and similarly for the lateral dynamics.

CHARACTERISTIC EQUATION

The lift increment due to trailing edge blowing is relatively insensitive to the section angle-of-attack perturbations about an unstalled operating point. However, the section lift change due to a velocity perturbation is

$$\delta L = \delta(\tfrac{1}{2}\rho V^2 c\, c_\ell) = \tfrac{1}{2}\rho V^2 c \left(c_{\ell_\alpha} \delta\alpha + c_{\ell_\mu} \delta C_\mu + 2 c_\ell \frac{\delta V}{V} \right)$$

$$= \tfrac{1}{2}\rho V^2 c \left(\frac{\lambda}{V} c_{\ell_\alpha} + 2(c_\ell - C_\mu c_{\ell_\mu}) \right) \frac{\delta V}{V}$$

where $\delta\alpha = \lambda/V$ is the induced angle-of-attack change due to a section velocity increase. This lift force has a component in the plane of the disk (the induced drag), as well as normal to the disk plane. Hence the blowing influences only the rotor aerodynamic flap moments and hub forces due to inplane velocity perturbations of the hub. The handling qualities of the hovering helicopter longitudinal dynamics are determined primarily by the pitch damping derivative M_q and the speed stability derivative M_u (similarly the lateral dynamics depend primarily on the roll damping L_p, and the speed stability or dihedral effect L_v). The pitch and roll damping produced by the rotor are due to the time lag of tip-path plane tilt relative to the shaft during

angular motions of the helicopter. This tip-path plane tilt produces the aerodynamic moment necessary to precess the rotor disk to follow the shaft motion. The source of the rotor aerodynamic moment is the flap moment due to flapping velocity, in other words a blade lift change due to an angle-of-attack perturbation. Therefore M_q and L_p are not influenced greatly by the trailing edge blowing (there is a minor effect since pitch or roll about the helicopter center-of-gravity will produce an inplane hub velocity). The speed stability produced by the rotor is however due to the flap moments and hub forces which occur during inplane motions of the rotor hub. Therefore M_u and L_v are directly influenced by the trailing edge blowing of the circulation controlled rotor. With zero or low blowing, a forward velocity of the helicopter increases the blade lift on the advancing side and decreases it on the retreating side of the disk. The rotor responds with a rearward tilt of the tip-path plane, which produces a thrust vector tilt and a hub moment. The resulting pitch up moment on the helicopter is the speed stability derivative ($M_u > 0$). The equation above shows that blowing reduces section $\partial L/\partial V$, and that for sufficiently high blowing coefficient the lift can actually decrease due to an inplane velocity increase, resulting in negative speed stability. In summary, the principal invluence of blowing on the rotor stability derivatives is a change in the speed stability M_u and L_v, which are reduced for $C_\mu > 0$. For sufficiently high blowing, negative speed stability is possible ($M_u > 0$ and $L_v < 0$ correspond to positive speed stability). An expression for the speed stability derivative is given in the appendix.

The characteristic equation of the helicopter longitudinal dynamics is

$$s^3 - (X_u + M_q)s^2 + (X_u M_q - X_q M_u)s + gM_u = 0$$

The influence of the speed stability M_u on the three roots of this equation is sketched below. With no blowing the helicopter has positive speed stability, $M_u > 0$. Then the roots of the hover longitudinal dynamics consist of a stable real root due to the pitch damping M_q, and a mildly unstable long period oscillatory mode due to the speed stability. With a low level

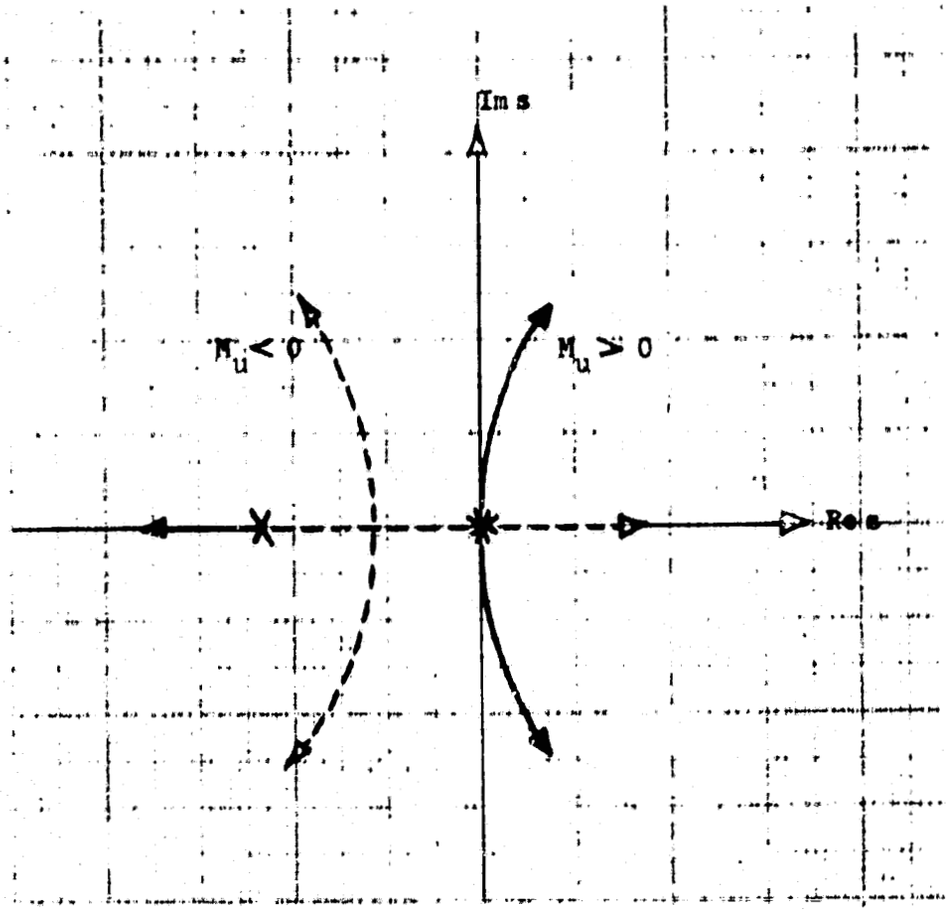

of blowing, the speed stability derivative M_u is reduced. The result is a reduction in the damping of the real root, and an increase in the period and time to double-amplitude of the oscillatory mode. This change in the oscillatory mode is favorable, and the influence on the real root will be small with a hingeless rotor. With sufficiently high blowing the rotor will have negative speed stability, $M_u < 0$. Then the roots of the hover dynamics consist of two stable real roots (or a stable oscillatory mode), and an unstable real divergence due to the speed stability. The time to double-amplitude of this unstable mode can be unacceptably short. There are similar effects of the blowing on the hovering helicopter lateral dynamics.

CALCULATED DYNAMIC CHARACTERISTICS

The calculated flight dynamics of the hovering helicopter with a circulation controlled rotor will be presented for the following example: rotor solidity $\sigma = 0.085$; blade Lock number $\gamma = 5$; mast height $h/R = 0.3$;

precone $\beta_p = 3^\circ$; pitch radius of gyration $(k_y/R)^2 = 0.10$; roll radius of gyration $(k_x/R)^2 = 0.04$; and a gravitational constant of $g/\Omega^2 R = 0.002$. A rotor speed of $\Omega = 27$ rad/sec is used to obtain dimensional results (hence with $g/\Omega^2 R = 0.002$, the rotor tip speed and radius are $\Omega R = 180$ m/sec and $R = 6.7$ m). The circulation controlled airfoil characteristics at constant Mach number were approximated by

$$c_\ell = a\alpha + bC_\mu^p$$

with $a = 7.0$, $b = 10.8$, and $p = 2/3$. For the blade section drag coefficient, $c_d = 0.012$ was used. The hover induced velocity was obtained using the momentum theory result $\lambda_o = k_h\sqrt{C_T/2}$, with the empirical factor $k_h = 1.15$. It was assumed that the blade section blowing coefficient varied inversely with the radial station along the span: $C_\mu = C_{\mu_t}(R/r)$. The flight dynamics are considered over a range of rotor lift (thrust coefficient to solidity ratios of $C_T/\sigma = 0.05$ to 0.15), as a function of the tip blowing coefficient C_{μ_t}. Several values of the flap frequency are considered: $\nu = 1$, as for a teetering or gimballed rotor; $\nu = 1.04$, representative of an offset-hinge articulated rotor; and $\nu = 1.09$ and 1.18, representative of hingeless rotors.

For a given value of the rotor lift, the collective pitch decreases as the blowing increases. Figure 1 shows the variation of θ_{75} with C_μ for the present example, at several levels of C_T/σ. A helicopter with a circulation controlled rotor would likely be operated by using the blowing to control C_T/σ, for a fixed value of geometric collective pitch. Figure 2 compares the solution for the coupled hover dynamics with the results of separate solutions of the decoupled equations for the longitudinal and lateral dynamics. The decoupled equations are lower order, hence easier to solve and easier to interpret. From figure 2 it is concluded that the solution of the decoupled equations contains the fundamental characteristics of the hovering helicopter flight dynamics. In particular, the behavior of the roots at high values of the blowing coefficient are correctly obtained.

Figure 3 shows the influence of trailing edge blowing on the calculated longitudinal flight dynamics in hover. The real and imaginary

parts of the roots are plotted as a function of the tip blowing coefficient C_{μ_t}; the right-hand axes show the corresponding time to double- or half-amplitude and period of the mode. Figures 3a and 3b give the roots for the articulated rotor ($\nu = 1$) and the hingeless rotor ($\nu = 1.09$) respectively, at several values of the rotor lift. Figure 3c gives the roots at $C_T/\sigma = 0.10$ for several values of the flap frequency. Figure 4 shows the influence of blowing on the lateral dynamics. The variation of the roots as the blowing coefficient increases follows the behavior sketched in the root locus above. Consider figure 3a. As C_{μ_t} increases from zero, the damping of the stable real root decreases while the damping and time to double-amplitude of the unstable oscillatory mode increase. At a value of C_{μ_t} which depends on the rotor lift, the two complex roots reach the origin, and for still higher C_{μ_t} become two real roots, one stable and one unstable. For this case of $\nu = 1.0$, the two stable real roots then meet on the real axis and break off to form a complex conjugate pair. With a hingeless rotor (figure 3b) the behavior is similar, except that the stable real root due to the pitch damping has much larger magnitude, and so does not combine with the other stable real root at high C_{μ_t}. Indeed this pitch root is off the scale of figures 3b and 3c, even for the offset-hinge articulated rotor ($\nu = 1.04$). The influence of blowing on the roots is similar for the lateral dynamics.

With a quasistatic rotor model, the effects of unsteady aerodynamics can be accounted for by using a lift deficiency function. The results shown in figures 3 and 4 were obtained using $C = 1$ for the lift deficiency function. However, the reduction of the rotor aerodynamic hub moments in hover due to the unsteady wake effects can be very large. Figure 5 shows the lift deficiency function variation with C_T/σ for the present example (see the appendix). Figures 6 and 7 present the results for the helicopter longitudinal and lateral dynamics including this lift deficiency function ($C < 1$). The influence of trailing edge blowing on the calculated dynamics is not significantly changed by including the lift deficiency function.

SPEED STABILITY

The point at which the complex roots reach the origin, and form a pair of real roots, corresponds to zero speed stability ($M_u = 0$ or $L_v = 0$). Examining figures 3 to 7, it is concluded that the value of C_{μ_t} for zero speed stability increases with C_T/σ and $\bar{\nu}$, is not sensitive to the lift deficiency function, and is the same for the longitudinal and lateral motions. Note that the unstable real root initially increases very quickly after this critical C_{μ_t} is reached, especially with low loading or an articulated rotor. Therefore the blowing coefficient can not be increased much above this point before the time to double-amplitude becomes unacceptably small.

Figure 8 shows the variation of the speed stability derivative M_u with the tip blowing coefficient C_{μ_t} and the rotor lift C_T/σ. Figure 9 shows the zero speed stability boundary on the C_T/σ vs. C_{μ_t} plane, as a function of flap frequency. The influence of the lift deficiency function is negligible for the $\bar{\nu} = 1.0$ boundary, and small for the $\bar{\nu} = 1.09$ boundary. For a high enough blowing coefficient, or a small enough rotor lift, the helicopter will have negative speed stability and hence an unstable real root for the hover dynamics. Figures 10 and 11 give the corresponding results with a pitch/flap coupling of $K_p = 0.5$; there is a small unfavorable influence of pitch/flap coupling. The speed stability derivatives depend primarily on the rotor aerodynamic flap moment due to the hub inplane velocity, M_μ. An estimate of the boundary for zero speed stability can be obtained from $M_\mu = 0$, which is also shown in figures 9 and 11 (see the appendix). With an articulated rotor the critical blowing for zero speed stability is significantly lower because the direct inplane hub force due to hub velocity (H_μ) decreases faster with C_{μ_t} than M_μ does. With hingeless rotors the influence of H_μ is much less than that of M_μ, so the criterion $M_\mu = 0$ gives a better estimate of the boundary.

CONTROL CHARACTERISTICS

The response of the helicopter longitudinal velocity $\dot{x}_F$ to cyclic pitch or blowing control has two zeros, a complex conjugate pair of relatively large magnitude. The pitch angle θ_F has a single real zero of very small magnitude. The zeros of the lateral response to control are similar. The zeros of the response to cyclic blowing δ_{1s} are identical to the zeros of the response to cyclic pitch θ_{1s} if $(X_{\delta_s} M_{\theta_s})/(X_{\theta_s} M_{\delta_s}) = 1$, which is exactly satisfied with $\nu = 1.0$, and is satisfied within 10% for $\nu > 1$. Calculations of the zeros for the numerical example considered above confirm that the zeros for cyclic blowing and cyclic pitch are essentially identical. Hence it is only the pole configuration which influences the helicopter response to control.

A conventional helicopter has a mildly unstable long period oscillation in hover, but the motion can be stabilized by the pilot with rate plus proportional feedback of the pitch motion ($\theta_{1s} = -K_\theta(\tau s + 1)\theta_F$), and similarly for the lateral dynamics. The root locus for such feedback is sketched below. The θ_F/θ_{1s} response has a single zero at the origin, and the lead adds another at $s = \tau^{-1}$. With a hingeless rotor the control power and damping of the rotor are high, and the lead τ required is not long. A moderate level of blowing will improve the helicopter control characteristics by reducing the speed stability. Blowing large enough to produce negative speed stability radically alters the pole configuration

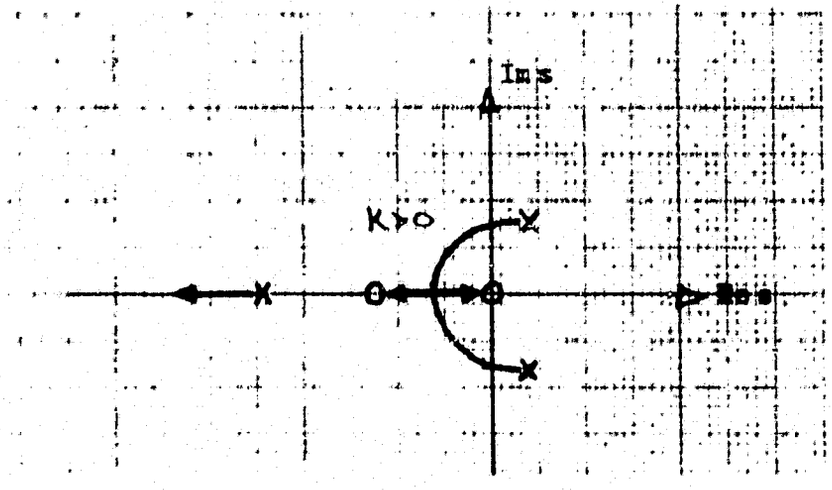

however. In this case, as sketched below, rate plus proportional feedback of the pitch attitude ($\delta_{1s} = -K_\theta(\tau s + 1)\theta_F$) improves the dynamic characteristics by increasing the time to double amplitude of the real divergence, but it does not completely stabilize the system regardless of the value of the lead τ. To obtain a stable system, feedback of the velocity perturbation could be added to counter the negative speed stability, and then rate plus proportional feedback of pitch used ($\delta_{1s} = -K_\theta(\tau s + 1)\theta_F + K_x \dot{x}_F$). Alternatively, integral feedback of pitch could be used as well to produce a stable system ($\delta_{1s} = -K_\theta((\tau_I s)^{-1} + 1 + \tau_R s)\theta_F$). Such control laws would likely be too complex for the pilot to comfortably handle. In any case, an automatic stability augmentation system is clearly desirable with

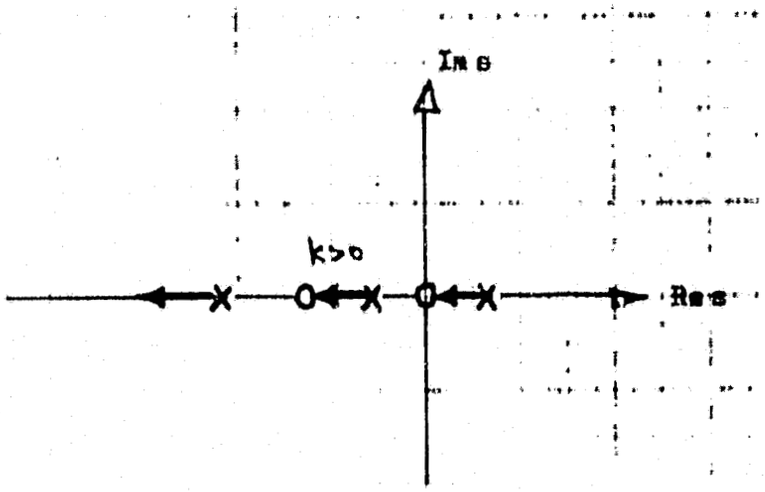

negative speed stability. Little work has been done on the handling qualities of helicopters with negative speed stability. Limited data in reference 2 indicates that the handling qualities are probably unacceptable if M_u is less than about -0.01 (m-sec)$^{-1}$, and clearly it is desirable to have positive speed stability ($M_u \geq 0$).

CONCLUDING REMARKS

With a conventional rotor, an increase in the blade inplane velocity increases the dynamic pressure and increases the angle-of-attack of the section, thereby increasing the lift. With a circulation controlled rotor,

an inplane velocity increase reduces the blowing coefficient C_{μ_t}, and thus tends to reduce the lift. If the blowing is high enough that there is a net reduction in the blade lift for an inplane velocity increase, the dynamic behavior of the rotor is radically altered. For the hovering flight dynamics, there is a critical blowing level, above which the rotor produces a negative speed stability derivative. The handling qualities of a helicopter with negative speed stability are probably unacceptable without a stability augmentation system.

APPENDIX

HOVERING HELICOPTER SPEED STABILITY DERIVATIVE

The equations of motion for the helicopter rigid body degrees of freedom, rotor flap motion, hub reactions, and inflow perturbation were obtained from the aeroelastic analysis of reference 3. For the rotor only the flap motion was considered, specifically the tip-path plane tilt degrees of freedom β_{1c} and β_{1s}. For the flap mode shape rigid body rotation with no hinge offset was assumed in order to simplify the aerodynamic and inertial coefficients. Hingeless rotors were modelled by retaining an arbitrary flap frequency ν. Perturbations of the rotor induced velocity, linearly varying over the rotor disk, were included to account for the rotor unsteady aerodynamics. The influence of these inflow perturbations principally takes the form of a lift deficiency function C multiplying the aerodynamic coefficients. A quasistatic solution for the rotor flap response was used. The flapping velocity and acceleration terms were dropped and then the flap equations were solved for the tip-path plane tilt response. The flapping velocity terms were dropped from the hub reactions, and the solutions for β_{1c} and β_{1s} substituted. From the resulting expansion of the rotor low frequency response in terms of the perturbation body motion, the stability derivatives for the flight dynamics analysis were identified. The result for the speed stability derivative M_u is as follows.

$$M_u = \frac{\gamma}{k_y^2 \Omega} \frac{1}{2C_T/\sigma a} \left\{ \frac{\nu^2-1}{\gamma/8} \frac{1}{1+N_*^2} M_\mu \right.$$

$$+ \frac{l_u}{R} \frac{8M_\mu}{1+N_*^2} \left[\left(2 + \left(\frac{1}{C} - 1\right) N_* \frac{\nu^2-1}{\gamma/8}\right) \frac{C_T}{\sigma a} + \frac{\nu^2-1}{\gamma/8} \left(N_* \frac{\lambda_0}{4} + \frac{\beta_0}{6}\right) \right]$$

$$\left. - \frac{l_u}{R} \left(2\lambda_0 M_\mu - H_\mu\right) \right]$$

where

$$N_* = \frac{\nu^2 - 1}{\gamma C/8} + K_P$$

and the lift deficiency function (from reference 3) is:

$$C = \frac{1}{1 + (\sigma a \kappa_h^2)/(8\lambda_0)}$$

The lateral speed derivative is $L_v = -(k_y^2/k_x^2)M_u$. The parameters required in this expression are:

g	acceleration due to gravity
k_y	pitch radius of gyration
k_x	roll radius of gyration
Ω	rotor angular velocity
C_T	rotor thrust coefficient
σ	rotor solidity ratio
a	blade section lift-curve slope
ν	flap frequency (per rev, in the rotating frame)
γ	blade Lock number
h	rotor mast height
R	rotor radius
λ_0	induced velocity
β_0	blade coning angle

The momentum theory value for the induced velocity in hover is $\lambda_0 = \kappa_h \sqrt{C_T/2}$, where κ_h is an empirical constant.

The rotor aerodynamic coefficients M_μ and H_μ are respectively the flap moment and blade drag force due to inplane velocity of the hub (see reference 3). It is only through these aerodynamic coefficients that the trailing edge blowing influences the flight dynamics. To evaluate M_μ and H_μ, it was assumed that the blade has constant chord and linear twist (θ_{tw}), and that the blowing coefficient varied along the blade span as $C_\mu = C_{\mu_t}(R/r)$. The circulation controlled airfoil characteristics were approximated by $c_\ell = a\alpha + b C_\mu^p$. The results for M_μ and H_μ are:

$$M_\mu = \frac{2C_T}{\sigma a} + \frac{\lambda_0}{4} - \frac{pb\,C_{\mu_t}^p}{a(3-p)}$$

$$H_\mu = \lambda_0\left(\frac{3C_T}{\sigma a} - \frac{\theta_{tw}}{8} + \frac{3}{4}\lambda_0\right) + \frac{3C_q}{4a} + \frac{\lambda_0}{2}\frac{b}{a}C_{\mu_t}^p\left(\frac{1-2p}{1-p} - \frac{3}{3-p}\right)$$

and for the blade coning and collective pitch angles:

$$\beta_0 = \frac{\nu^2-1}{\nu^2}\beta_p + \frac{\gamma}{\nu^2}\left[\frac{3}{4}\frac{C_T}{\sigma a} + \frac{\theta_{tw}}{160} + \frac{\lambda_0}{48} - \frac{bp\,C_{\mu_t}^p}{a3(3-p)(4-p)}\right]$$

$$\theta_{75} = \frac{6C_T}{\sigma a} + \frac{3}{2}\lambda_0 - \frac{3b\,C_{\mu_t}^p}{a(3-p)}$$

where β_p is the hub precone angle.

The speed stability derivative depends primarily on the rotor aerodynamic coefficient M_μ. Hence an estimate of the boundary for zero speed stability can be obtained from $M_\mu = 0$, which gives

$$C_{\mu_t} = \left[\frac{\frac{2C_T}{\sigma a} + \frac{k_h}{4}\sqrt{\frac{C_T}{2}}}{bp/a(3-p)}\right]^{\frac{1}{p}}$$

or with a = 7.0, b = 10.8, p = 2/3, and k_h = 1.15:

$$C_{\mu_t} = (0.648\ C_T/\sigma + 0.461\sqrt{C_T}\ )^{1.5}$$

REFERENCES

1 Seckel, Edward, Stability and Control of Airplanes and Helicopters, Academic Press, New York, 1964

2 Kelly, James R., and Garren, John F., Jr., "Study of the Optimum Values of Several Parameters Affecting Longitudinal Handling Qualities of VTOL Aircraft," NASA TN D-4624, July 1968

3 Johnson, Wayne, "Aeroelastic Analysis for Rotorcraft in Flight or in a Wind Tunnel," NASA TN D-8518, July 1977

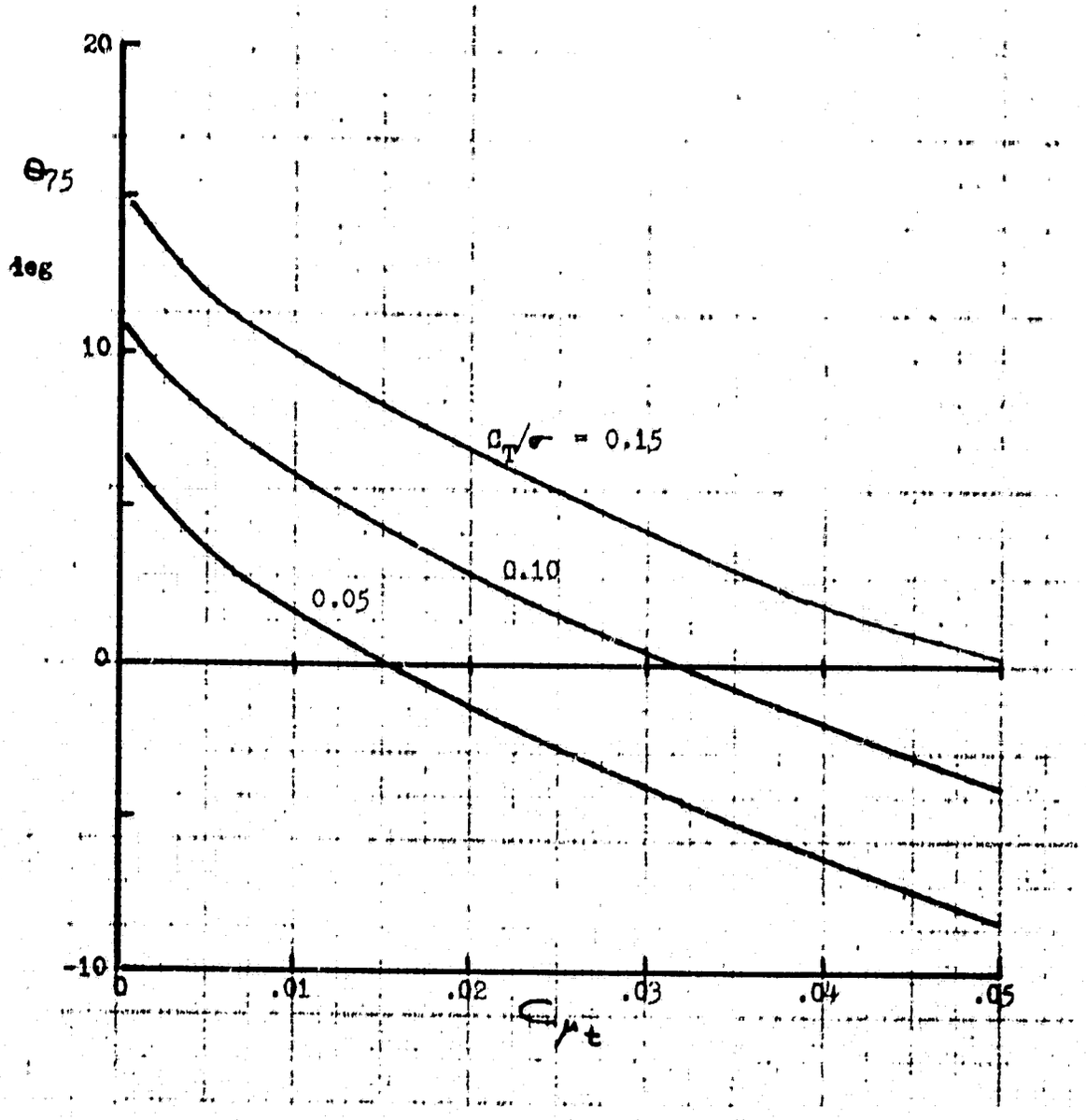

Figure 1 Rotor blade collective pitch as a function of rotor loading and blowing coefficient.

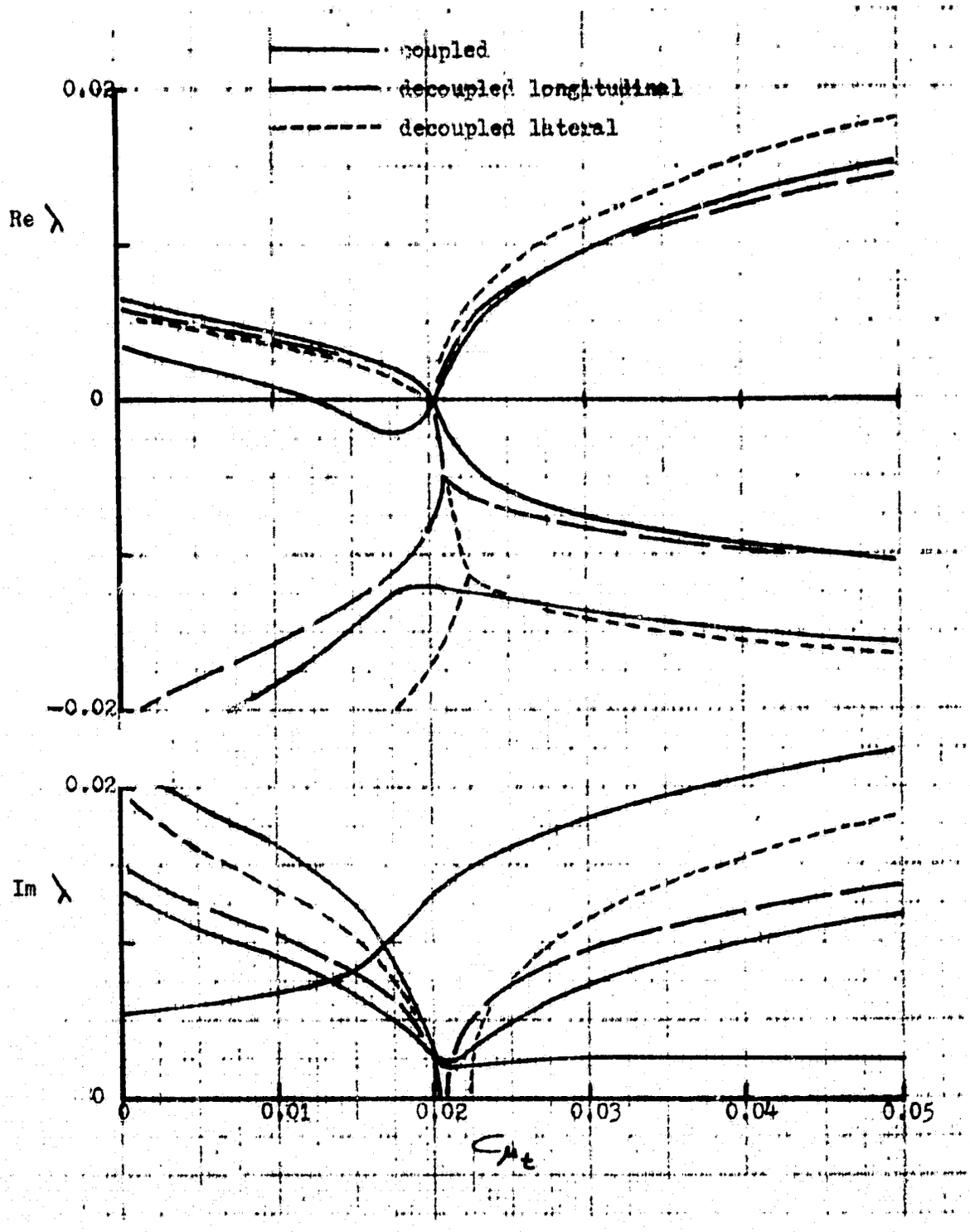

(a) Flap frequency ν = 1.0

Figure 2 Comparison of solutions of the coupled and decoupled equations of motion, at C_T/σ = 0.10.

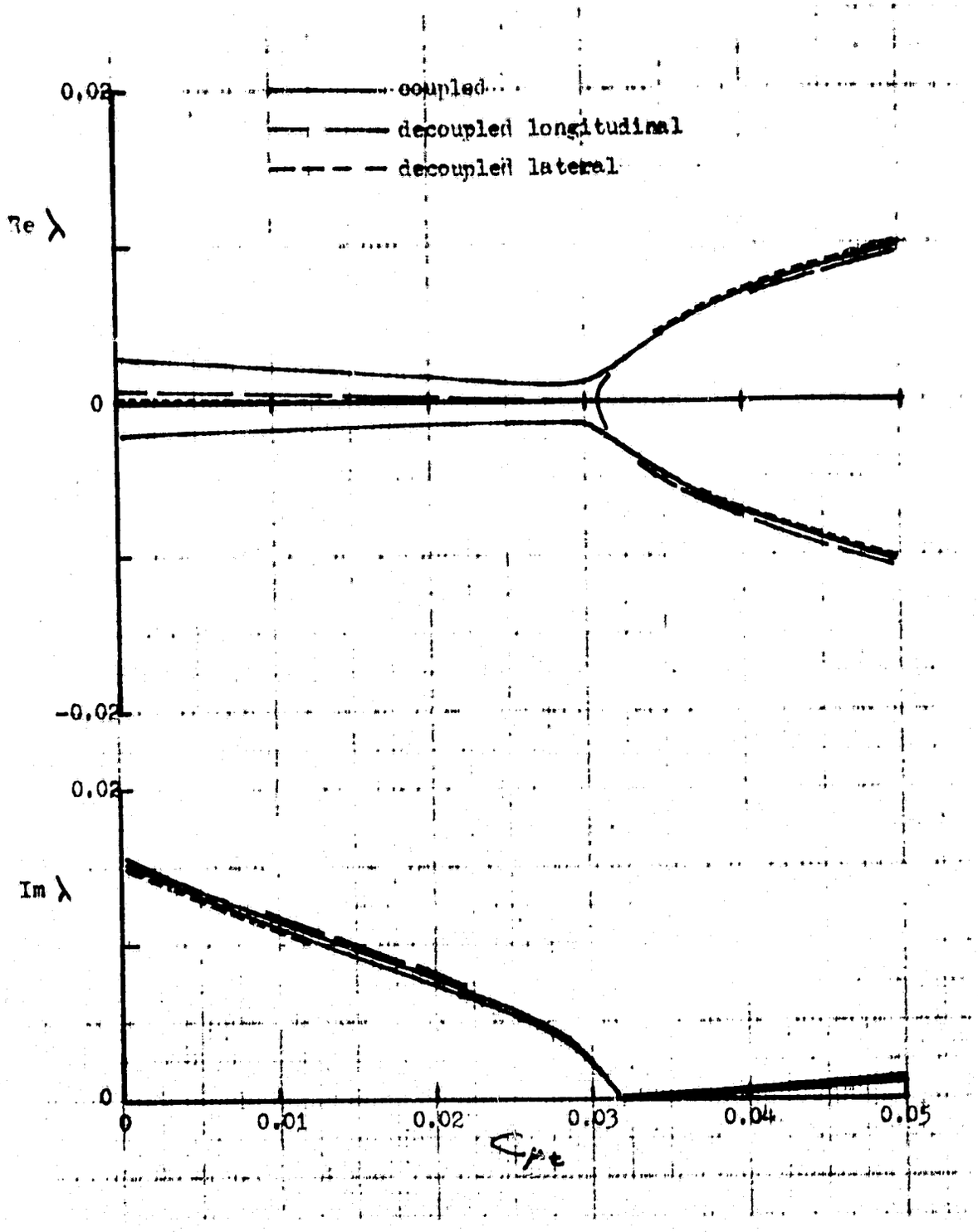

(b) Flap frequency $\nu = 1.09$

Figure 2 Concluded.

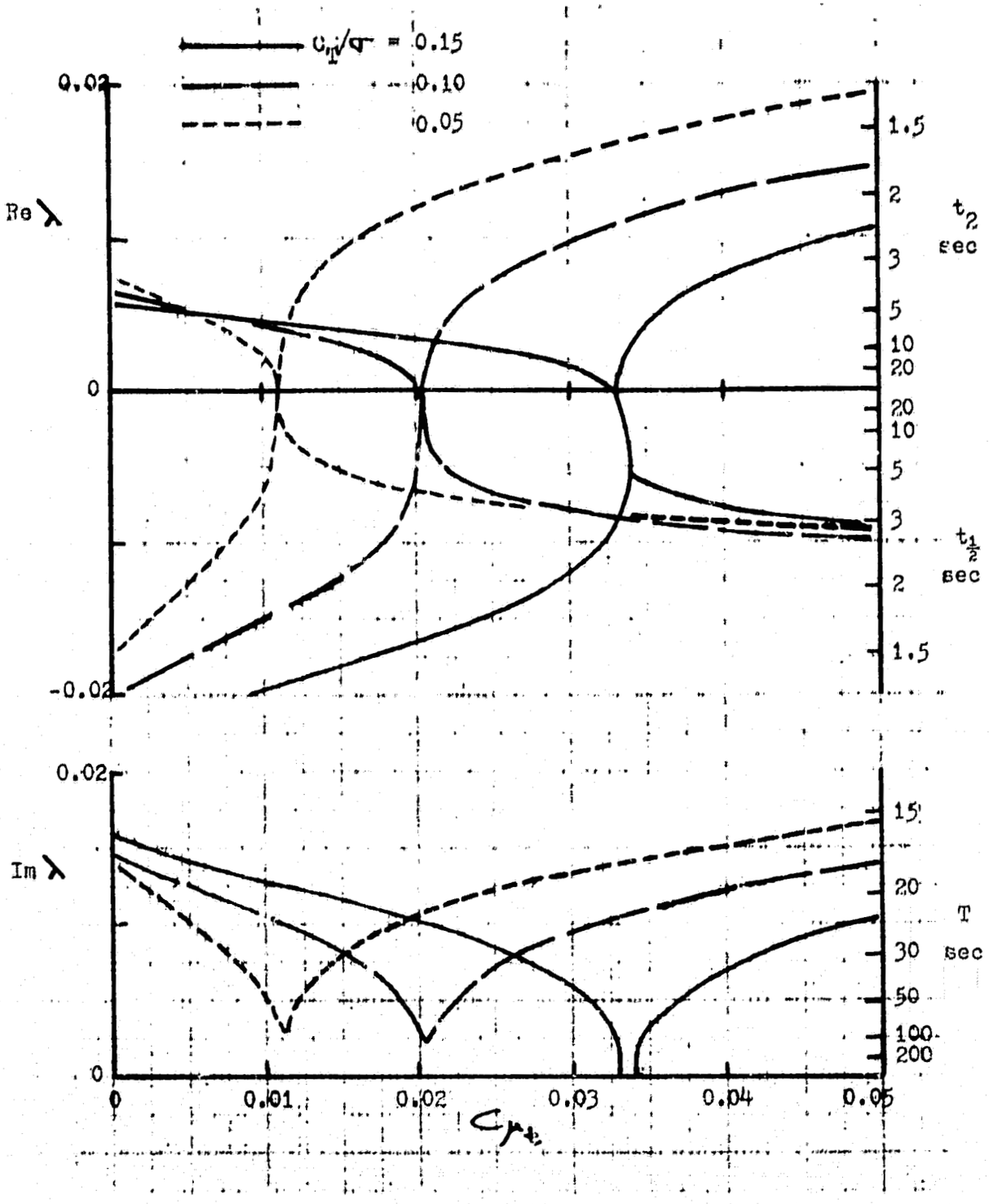

(a) Flap frequency ν = 1.0

Figure 3 Calculated roots of the hover longitudinal dynamics as a function of the tip blowing coefficient.

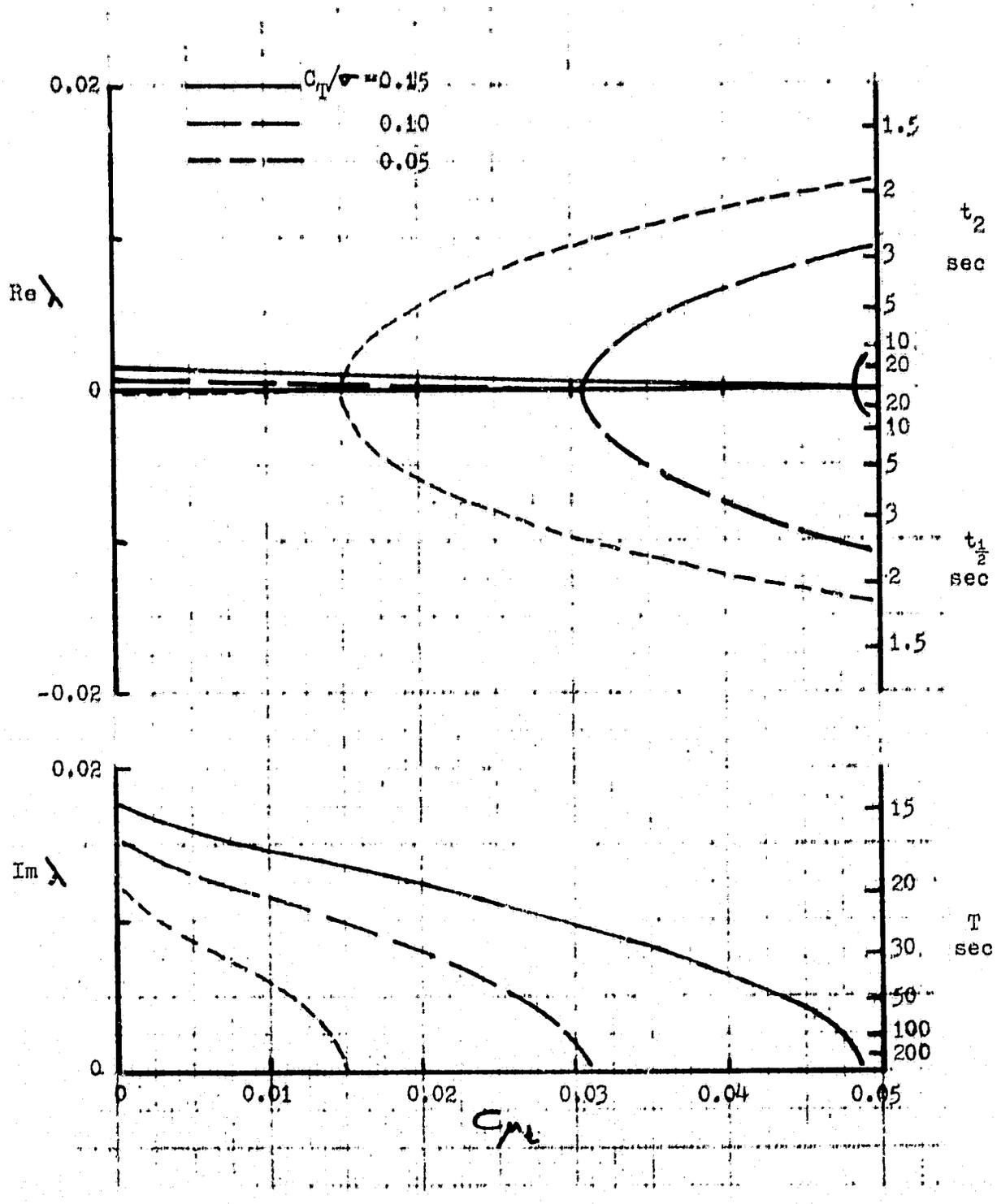

(b) Flap frequency ν = 1.09

Figure 3 Continued.

ORIGINAL PAGE IS
OF POOR QUALITY

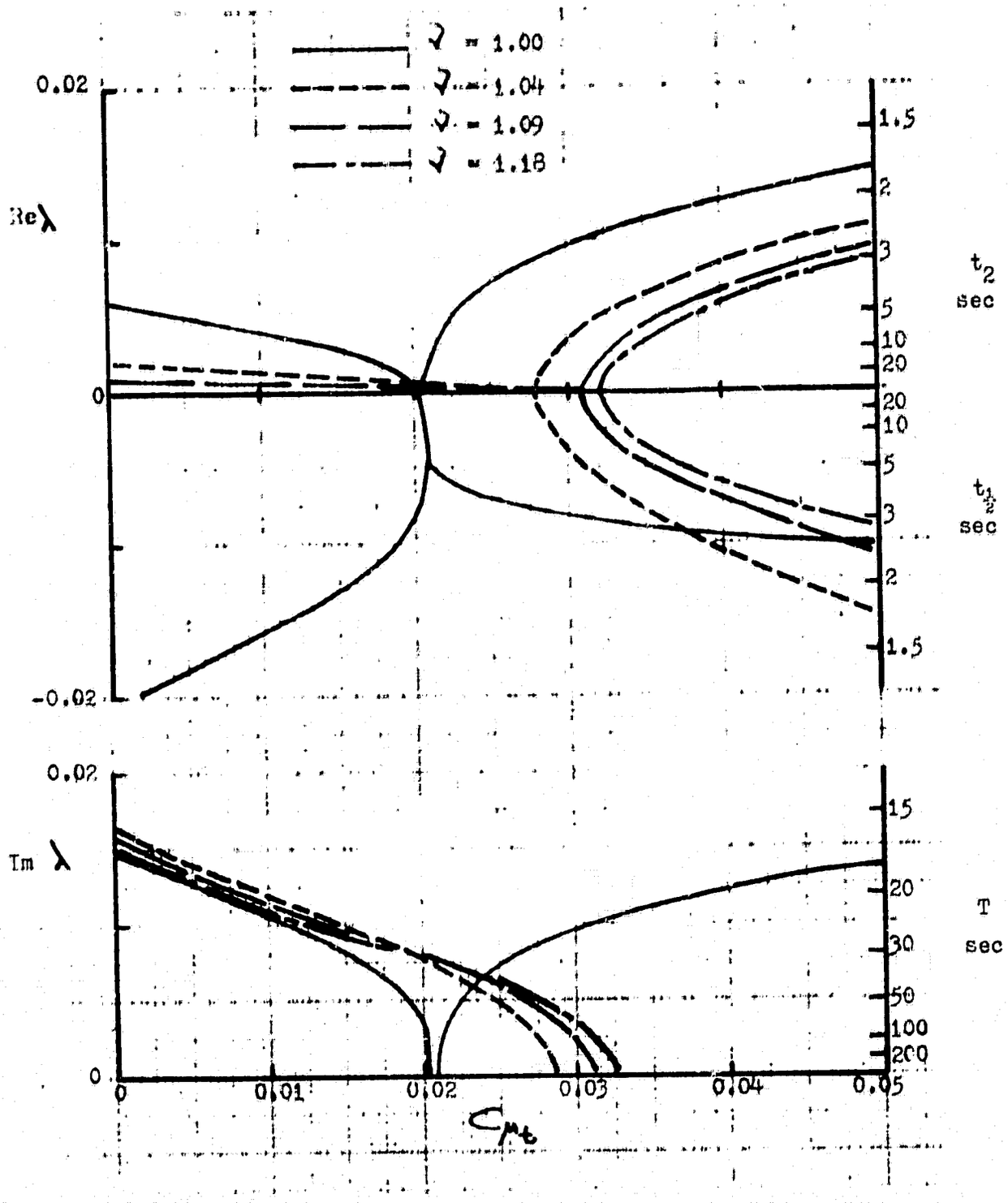

(c) Lift C_T/σ = 0.10

Figure 3 Concluded.

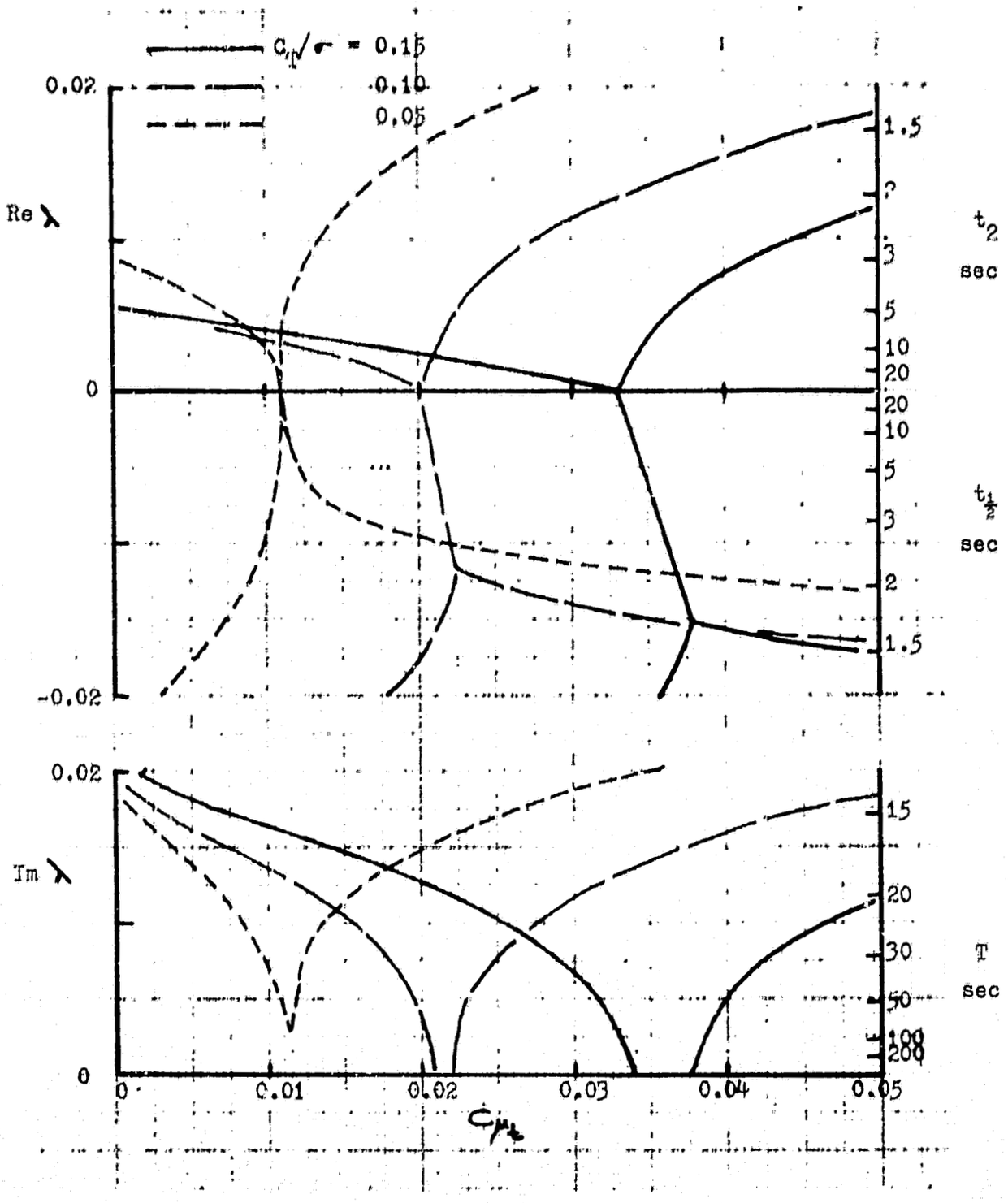

(a) Flap frequency ν = 1.0

Figure 4 Calculated roots of the hover lateral dynamics as a function of the tip blowing coefficient.

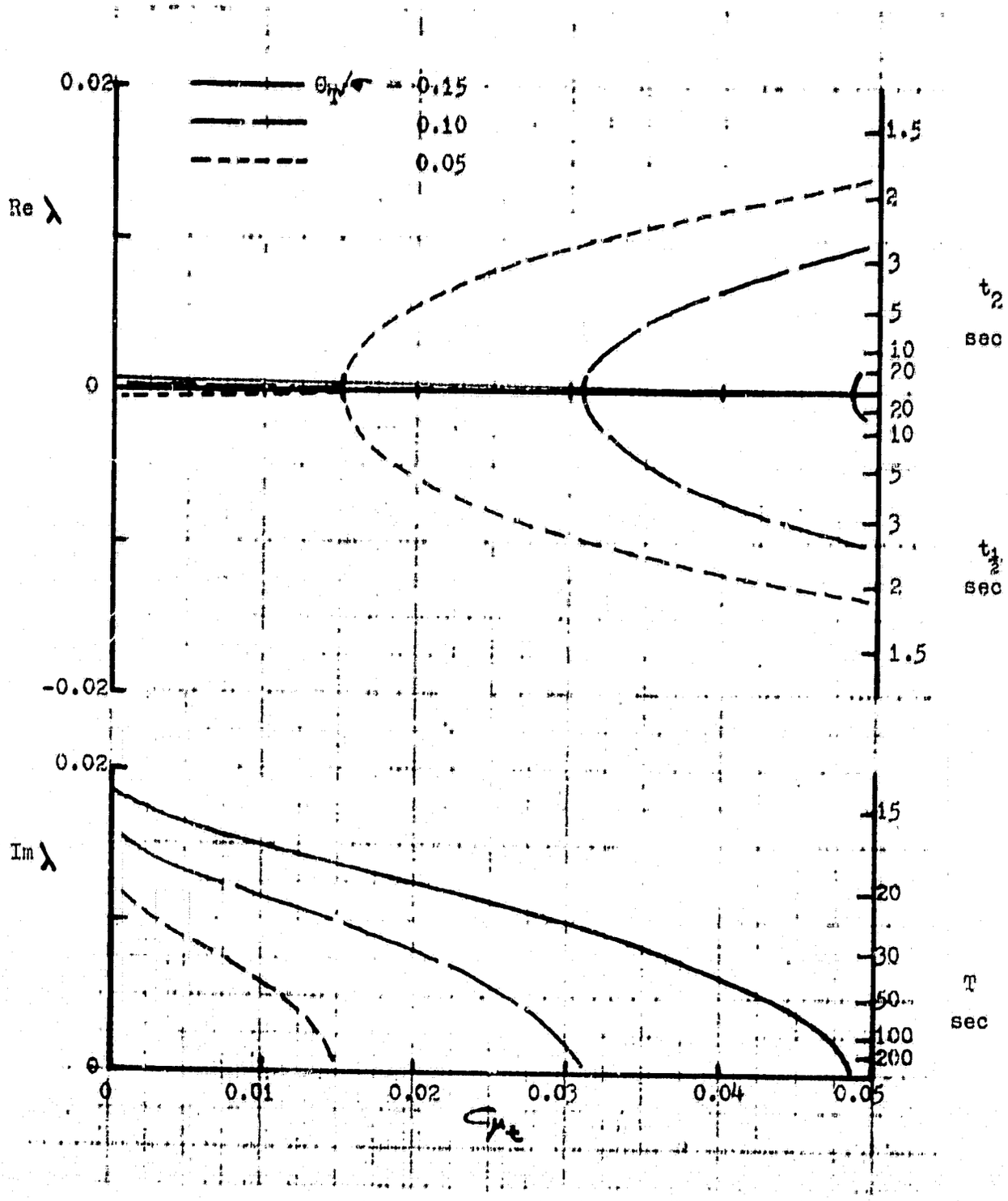

(b) Flap frequency Ω = 1.09

Figure 4 Continued.

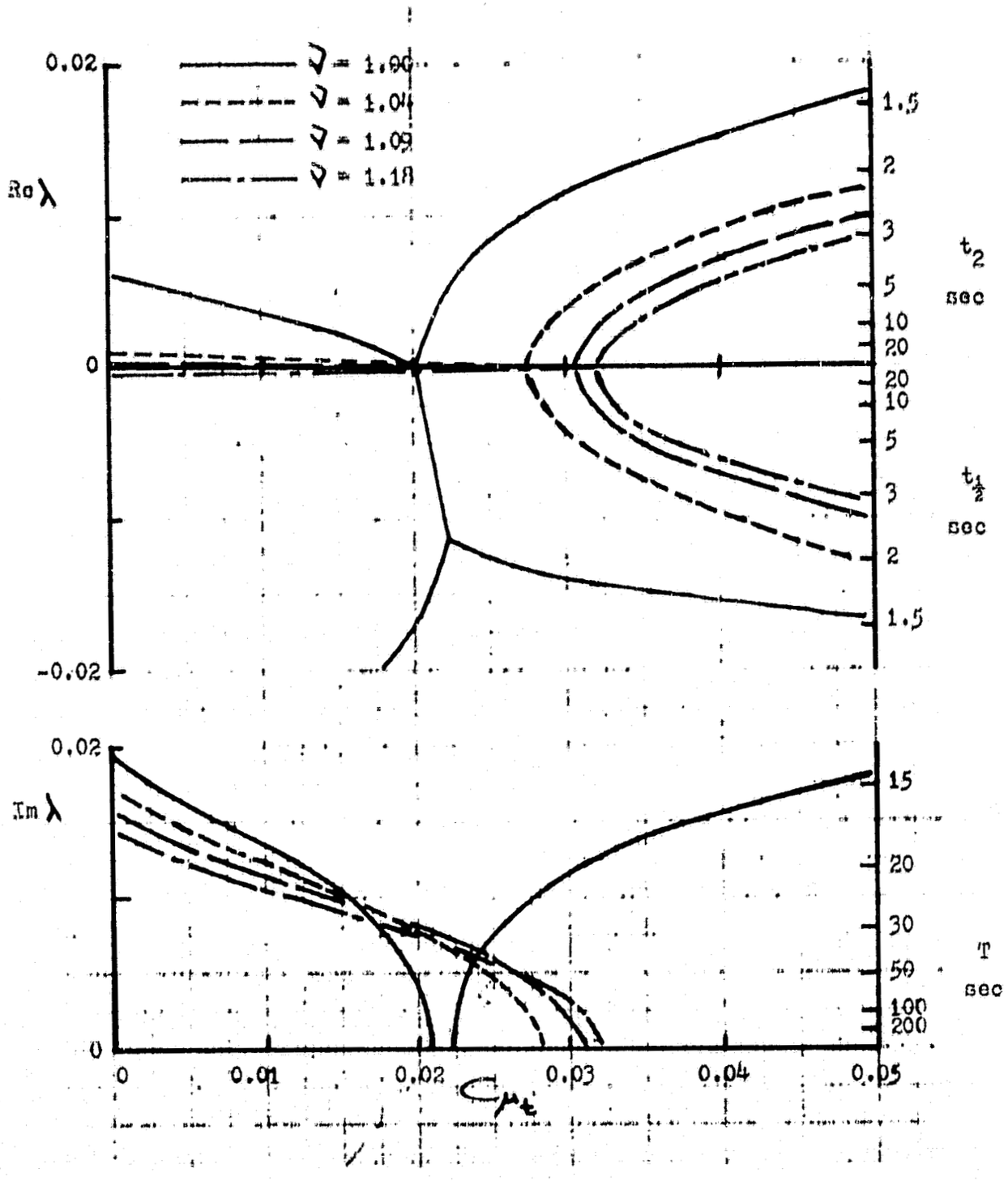

(c) Lift $C_T/\sigma = 0.10$

Figure 4 Concluded.

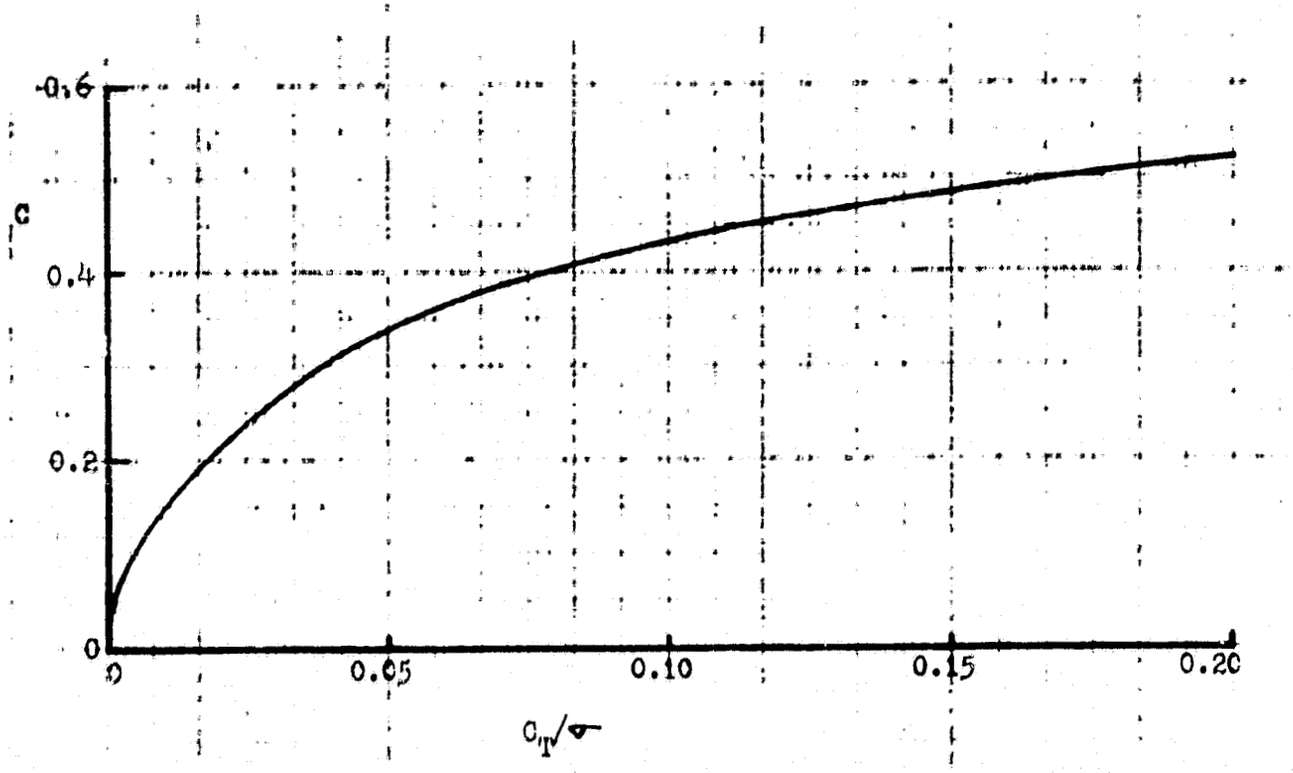

Figure 5 Lift deficiency function for rotor hub moments (σ = 0.085).

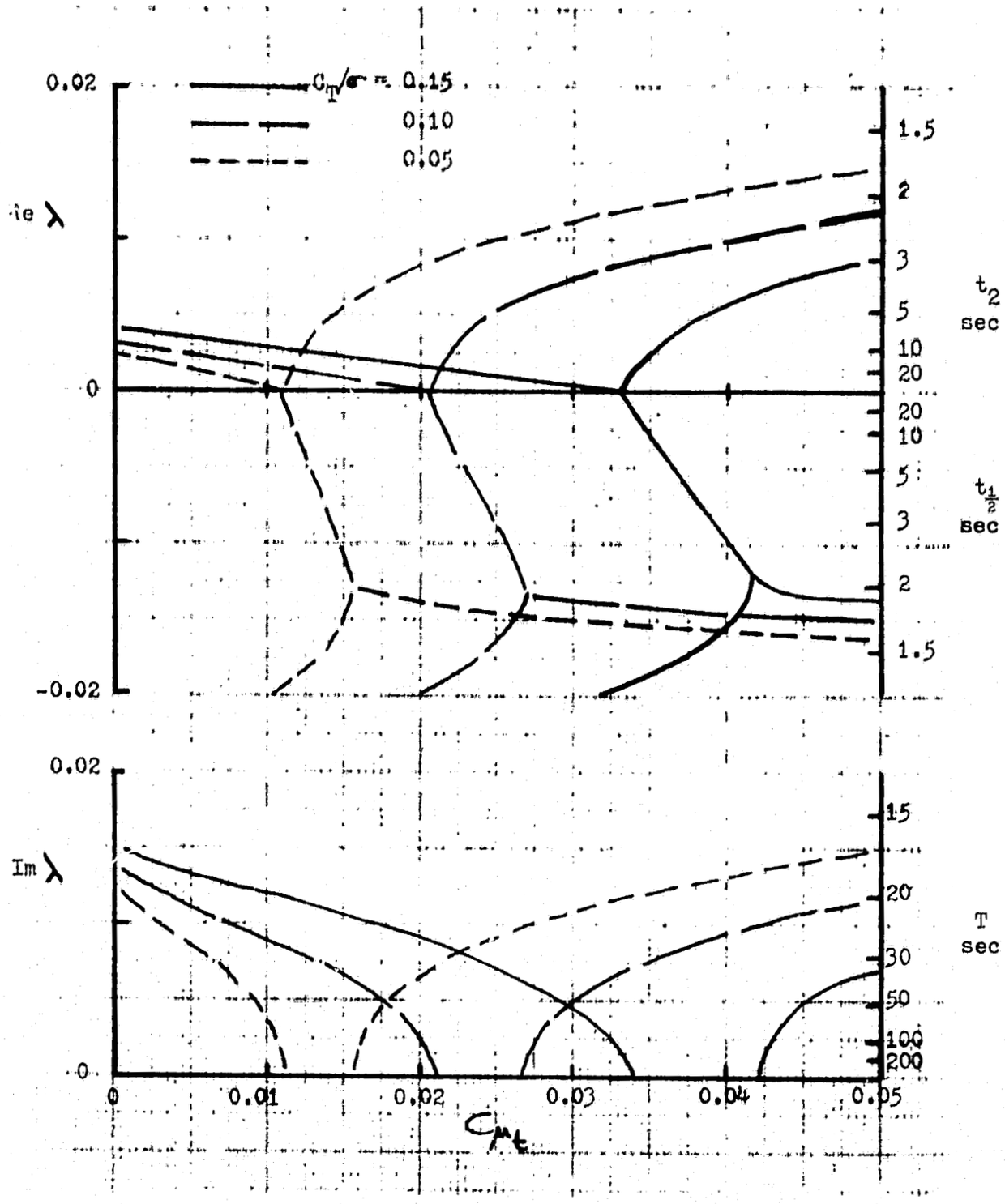

(a) Flap frequency $\mathcal{J} = 1.0$

Figure 6 Calculated roots of the hover longitudinal dynamics as a function of the tip blowing coefficient, including the lift deficiency function.

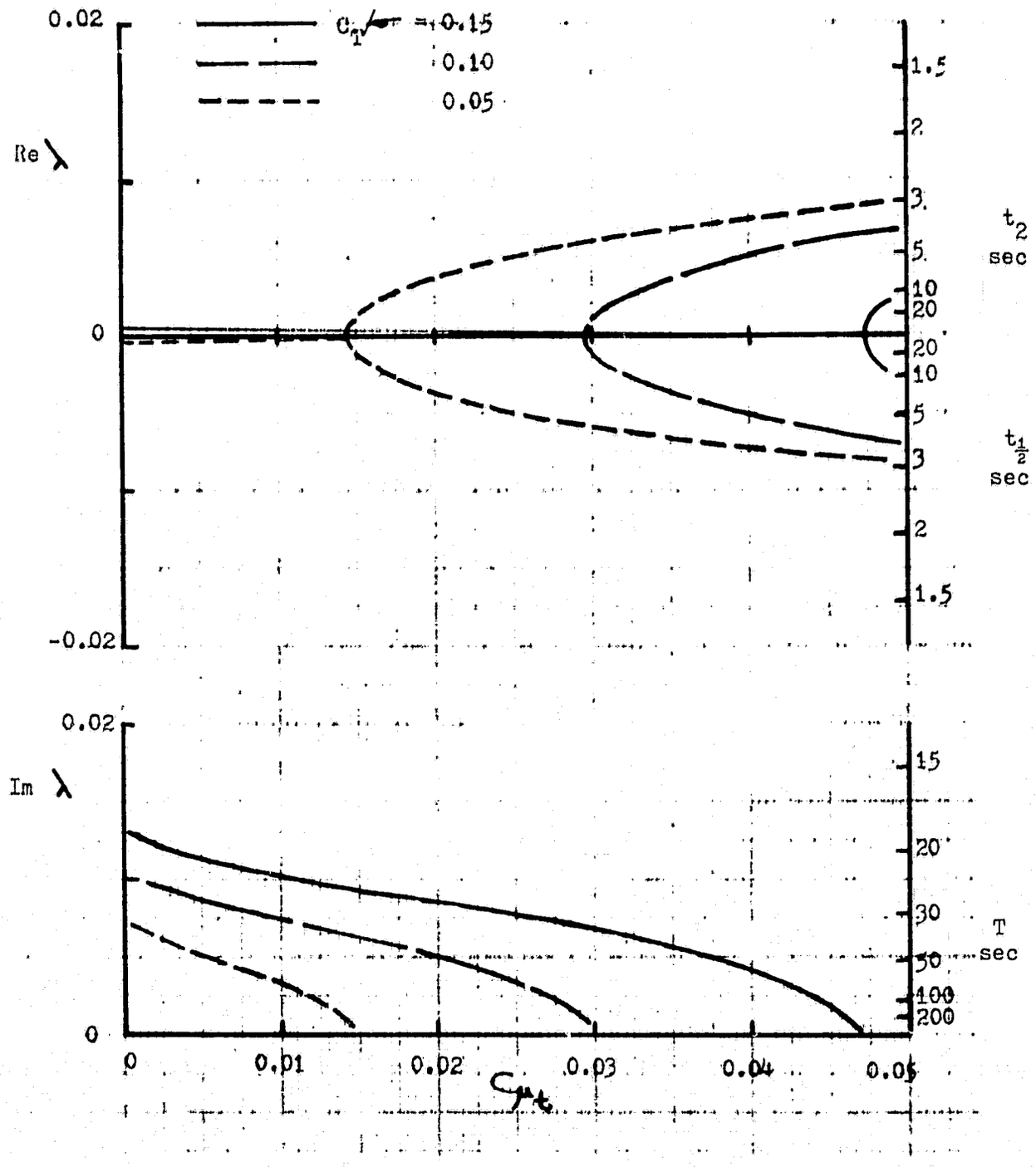

(b) Flap frequency ν = 1.09

Figure 6 Continued.

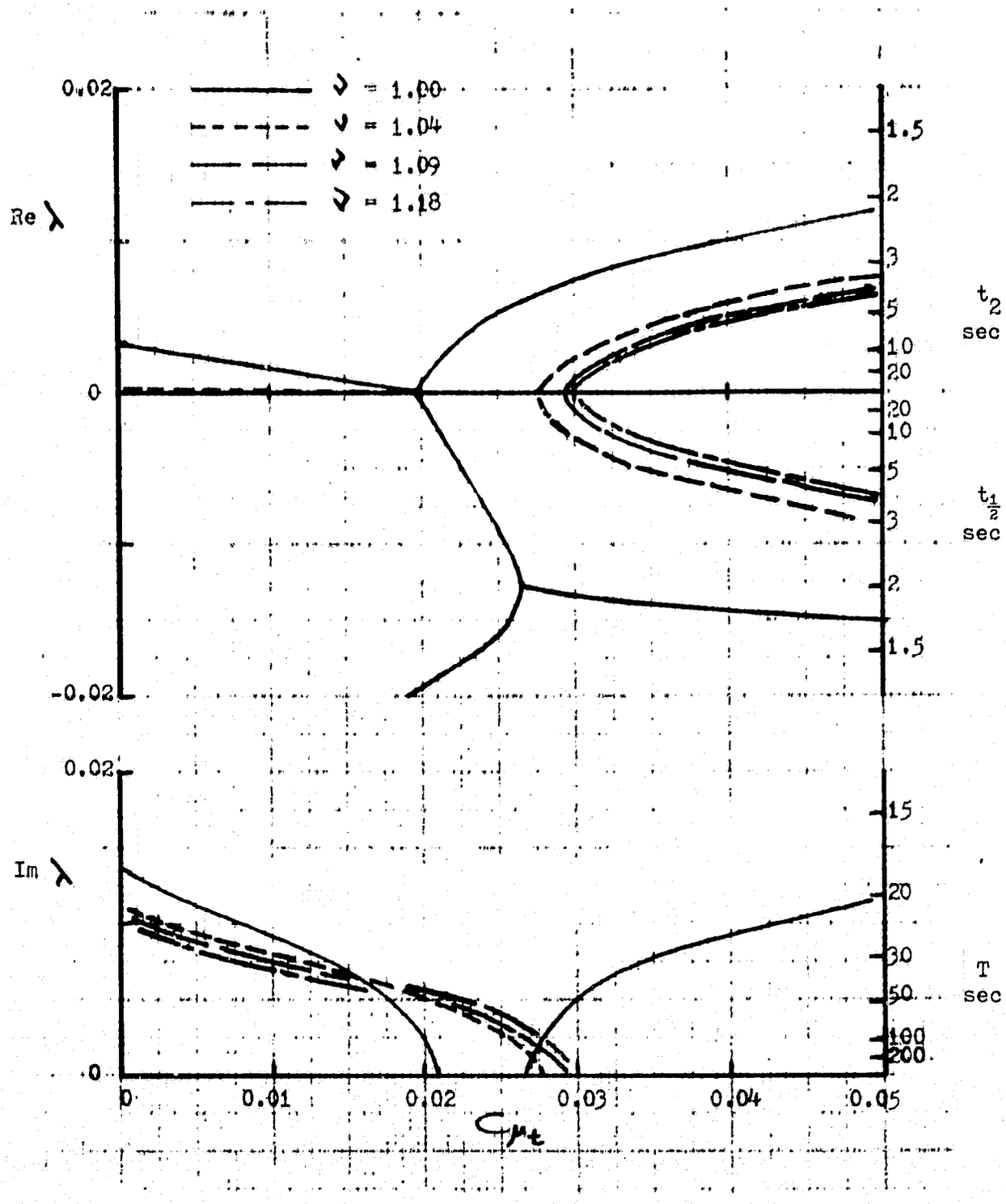

(c) Lift C_T/σ = 0.10

Figure 6 Concluded.

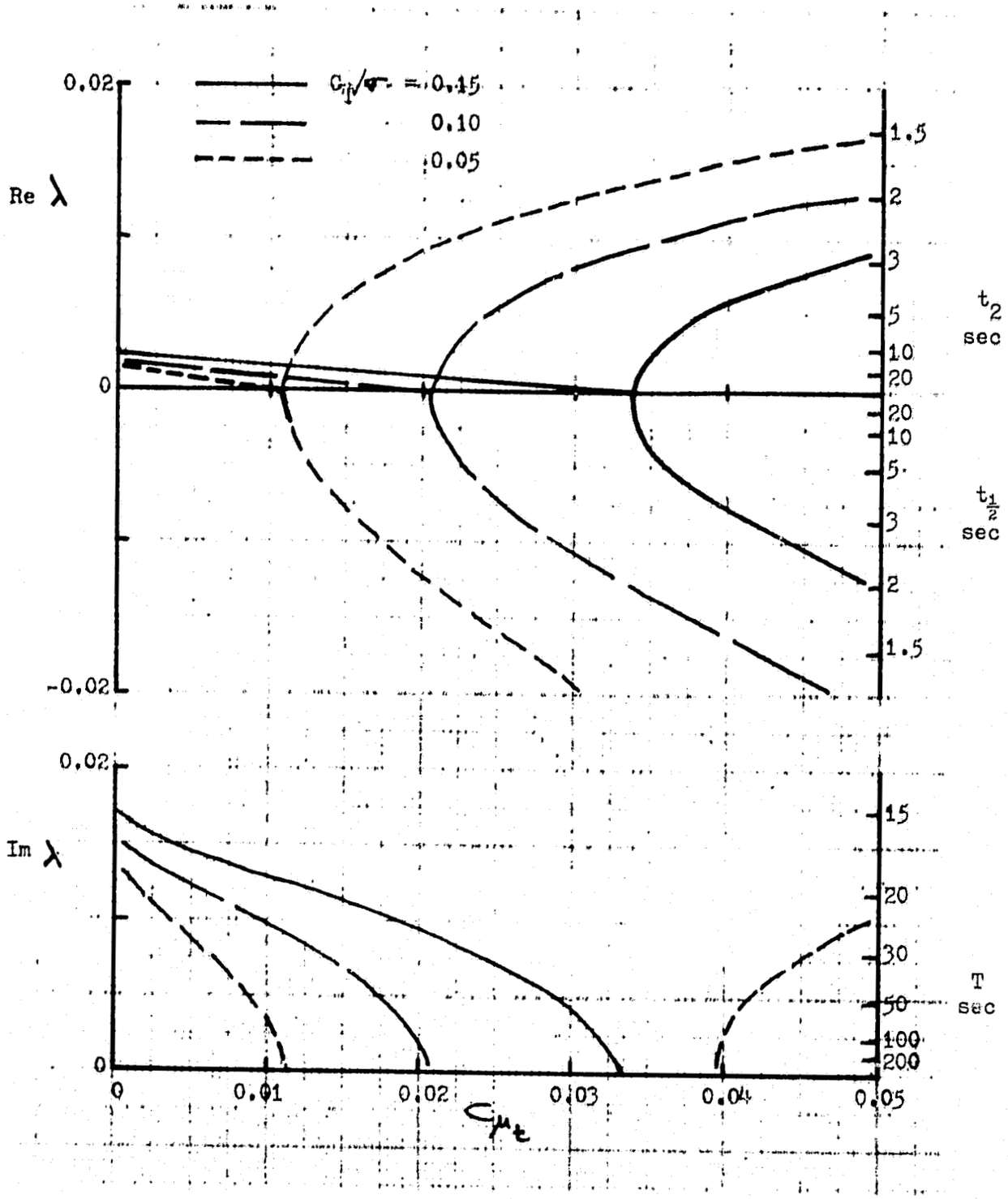

(a) Flap frequency $\nu = 1.0$

Figure 7 Calculated roots of the hover lateral dynamics as a function of the tip blowing coefficient, including the lift deficiency functiion.

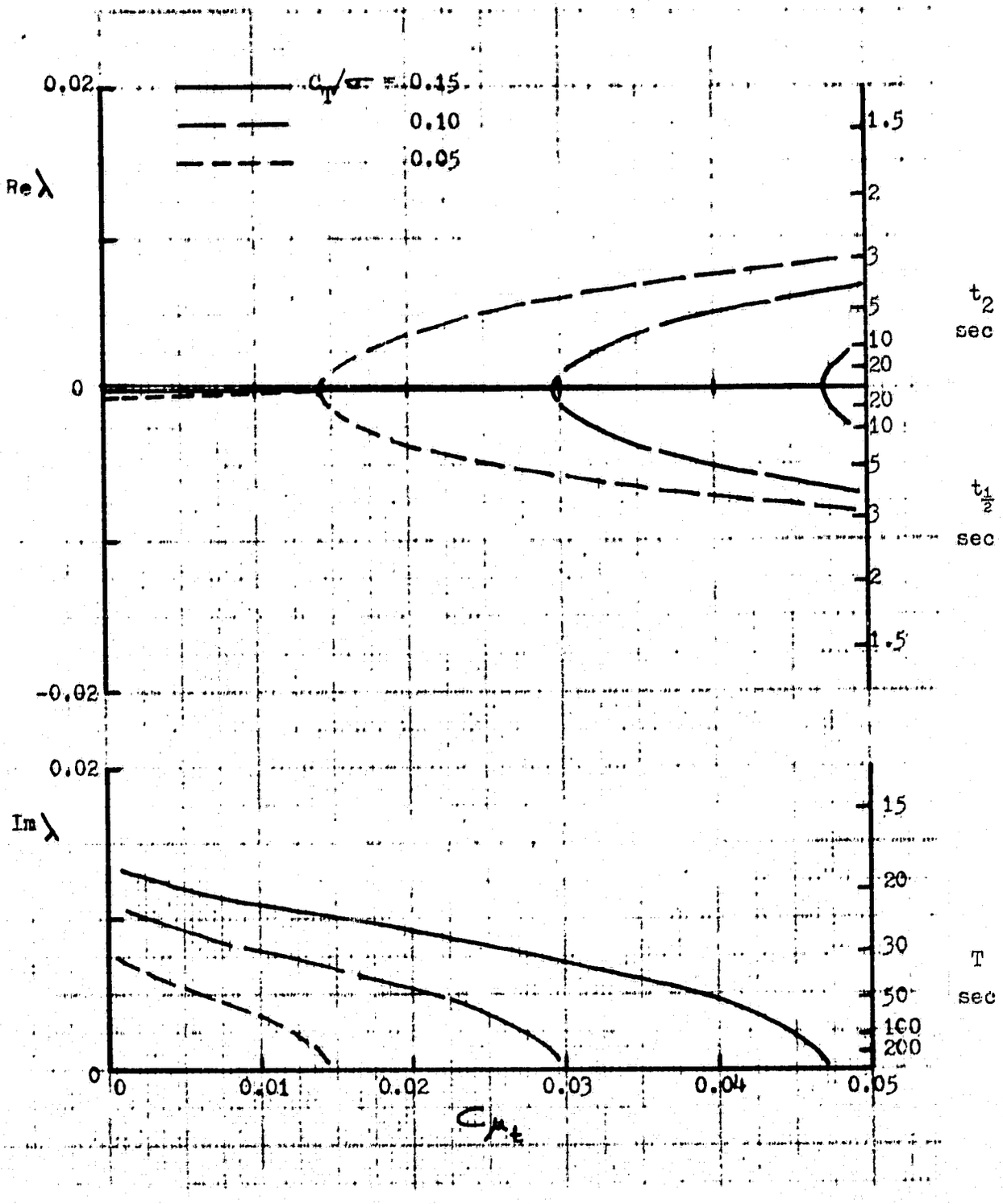

(b) Flap frequency ν = 1.09

Figure 7 Continued.

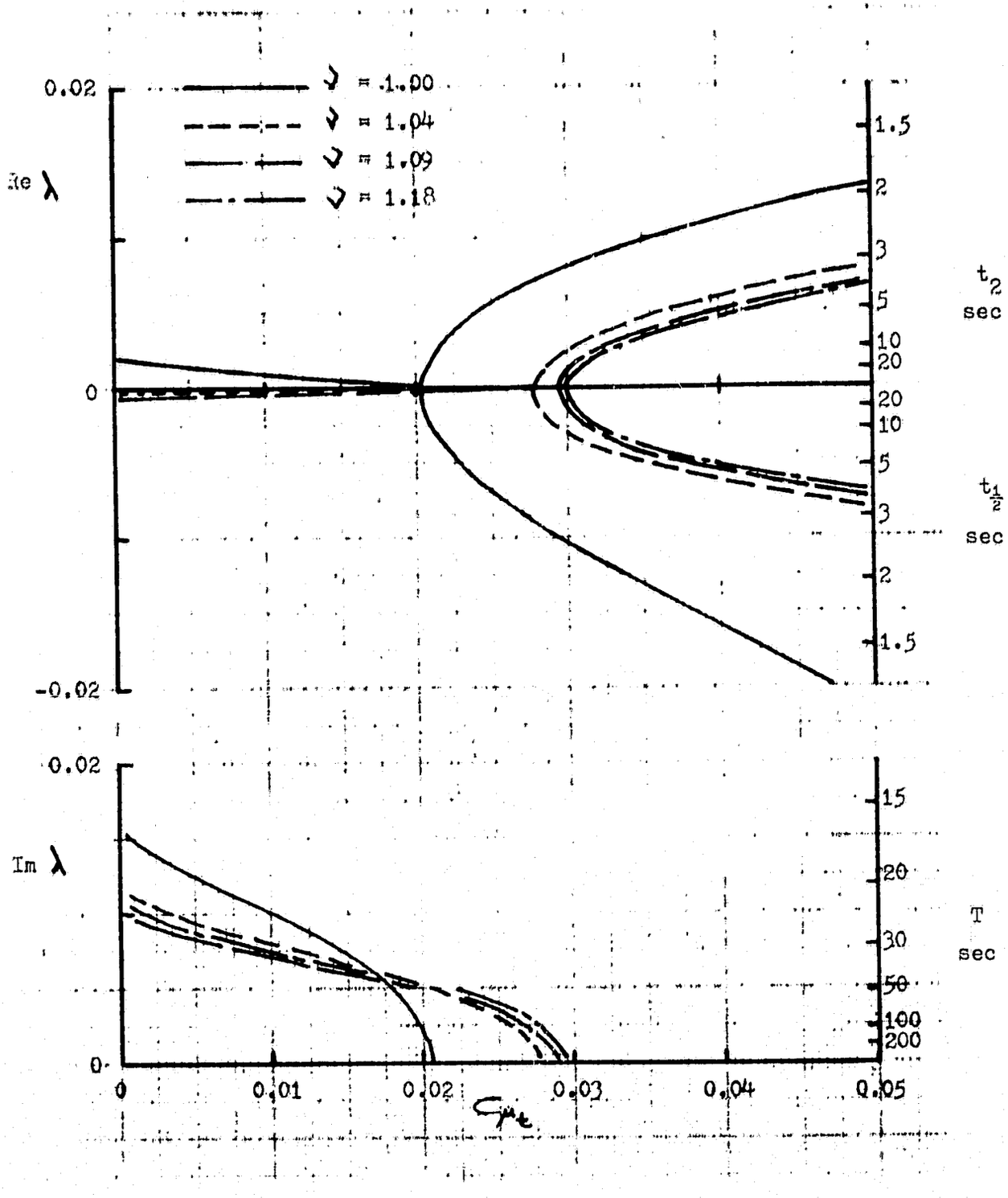

(c) Lift C_T/σ = 0.10

Figure 7 Concluded.

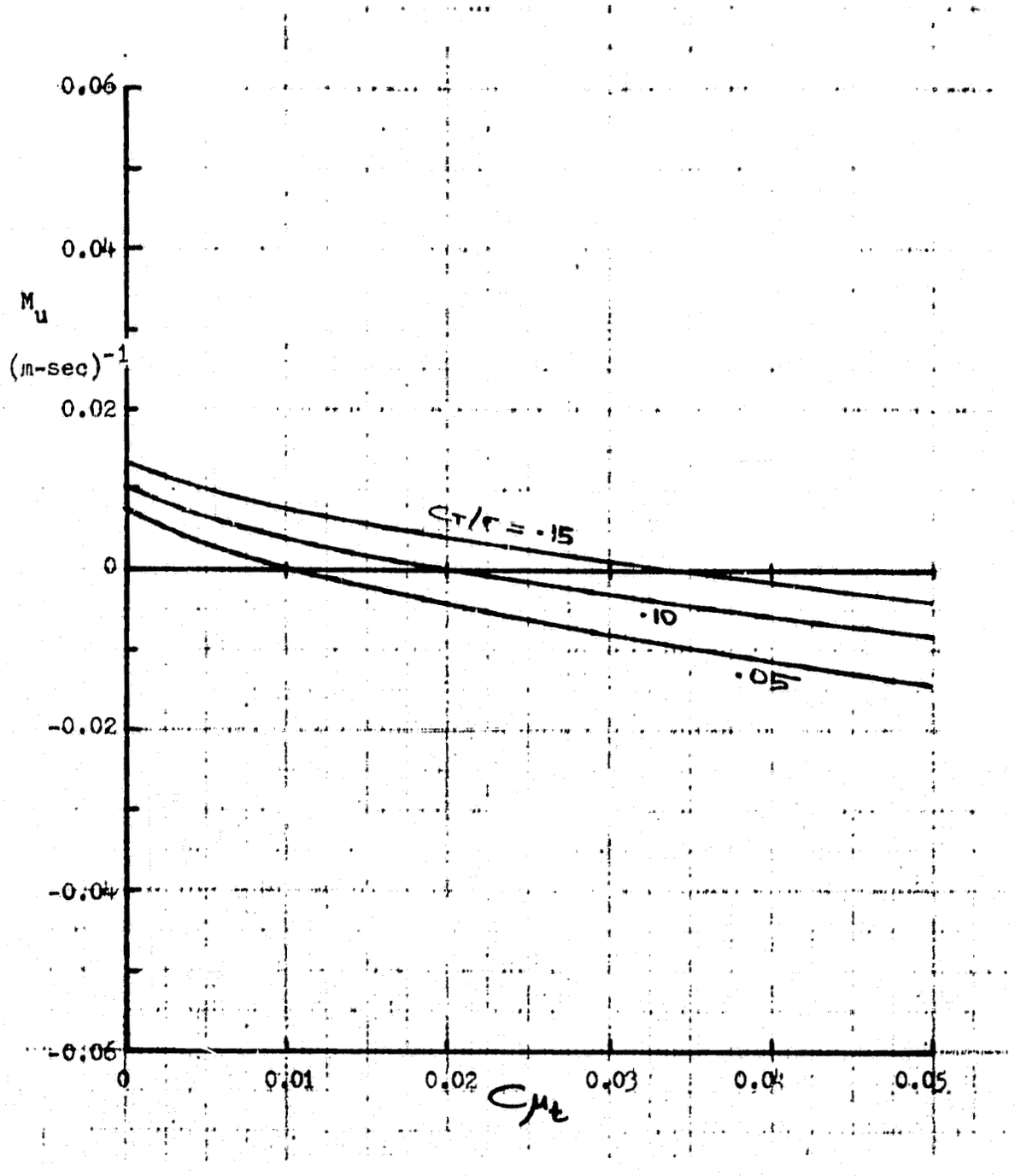

(a) Flap frequency $\nu = 1.0$ (negligible effect of the lift deficiency function).

Figure 8 Speed stability derivative M_u as a function of C_T/σ and C_{μ_t}.

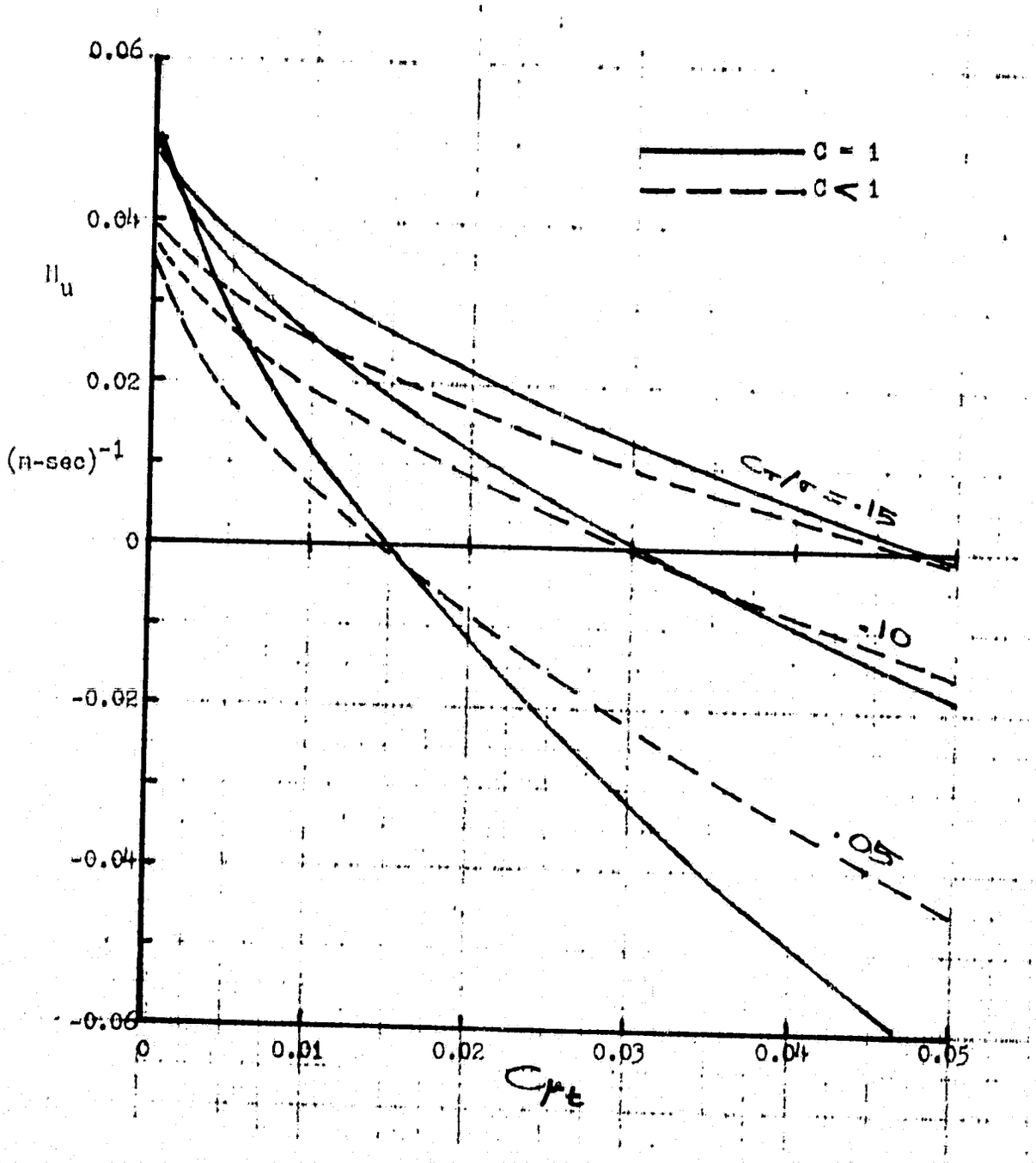

(b) Flap frequency ν = 1.09 (with and without lift deficiency function).

Figure 8 Concluded.

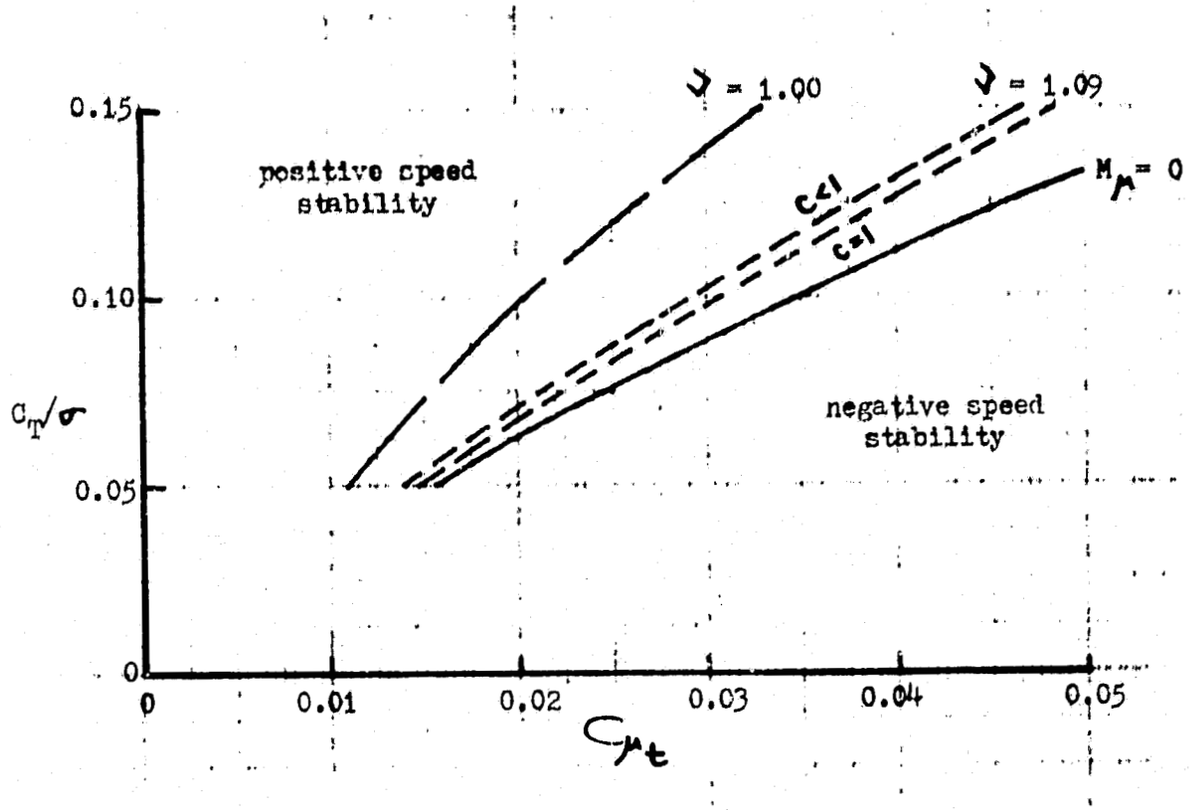

Figure 9 Boundary for zero speed stability (σ = 0.085).

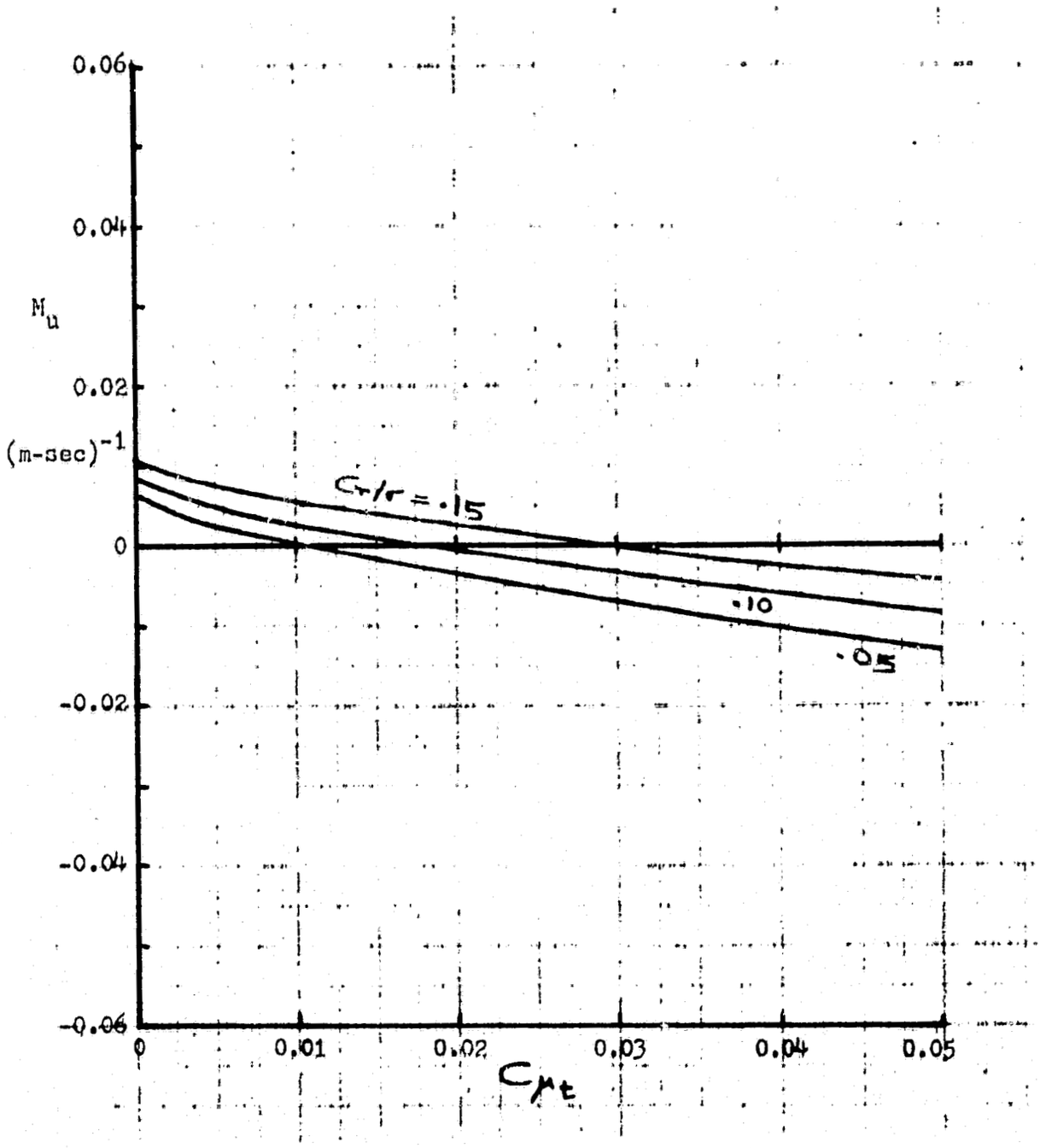

(a) Flap frequency $\nu = 1.0$ (negligible effect of the lift deficiency function)

Figure 10 Speed stability derivative M_u as a function of C_T/σ and C_{μ_t}, with pitch/flap coupling $K_p \cong 0.5$.

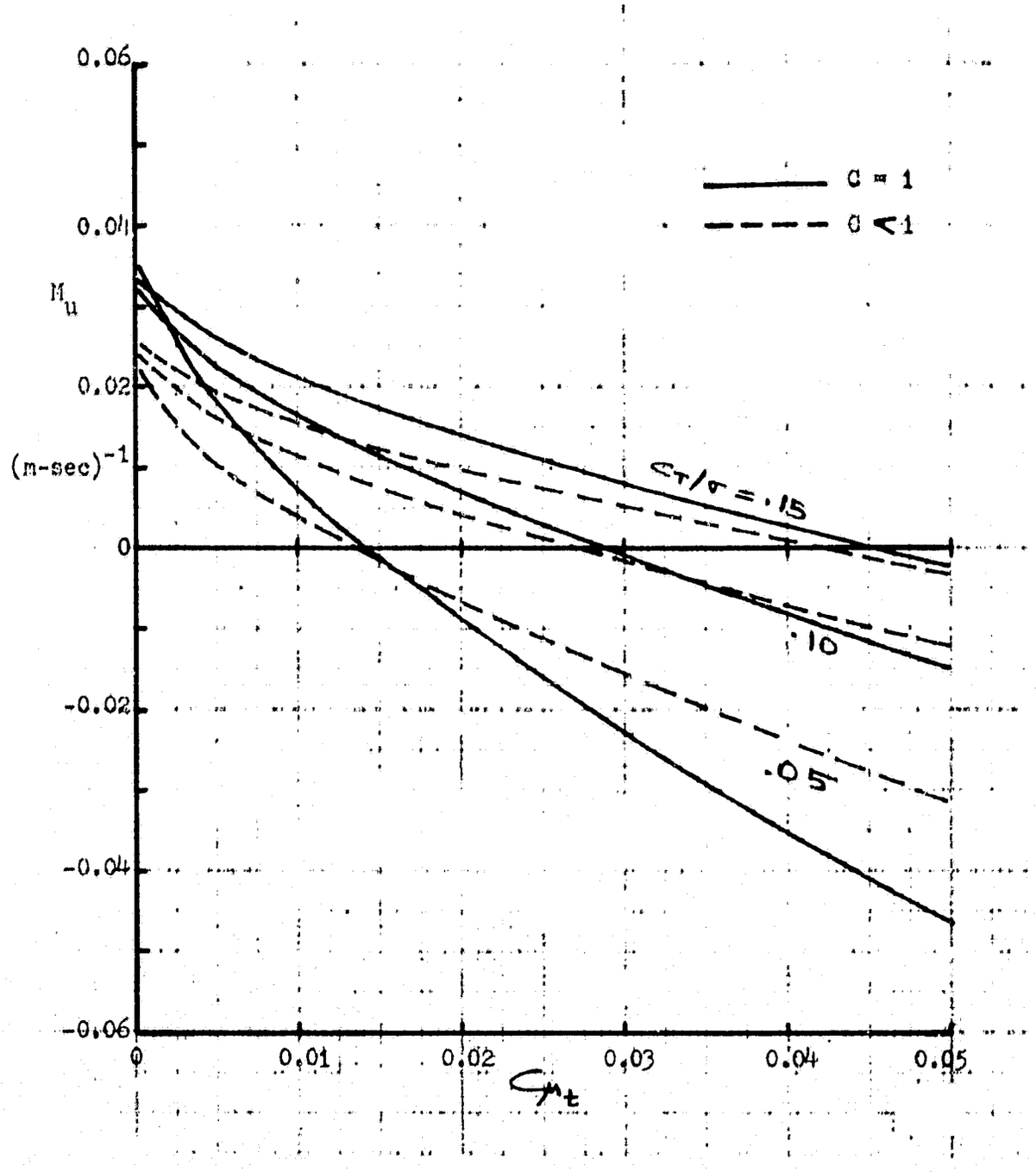

(b) Flap frequency $\nu = 1.09$ (with and without lift deficiency function)

Figure 10 Concluded.

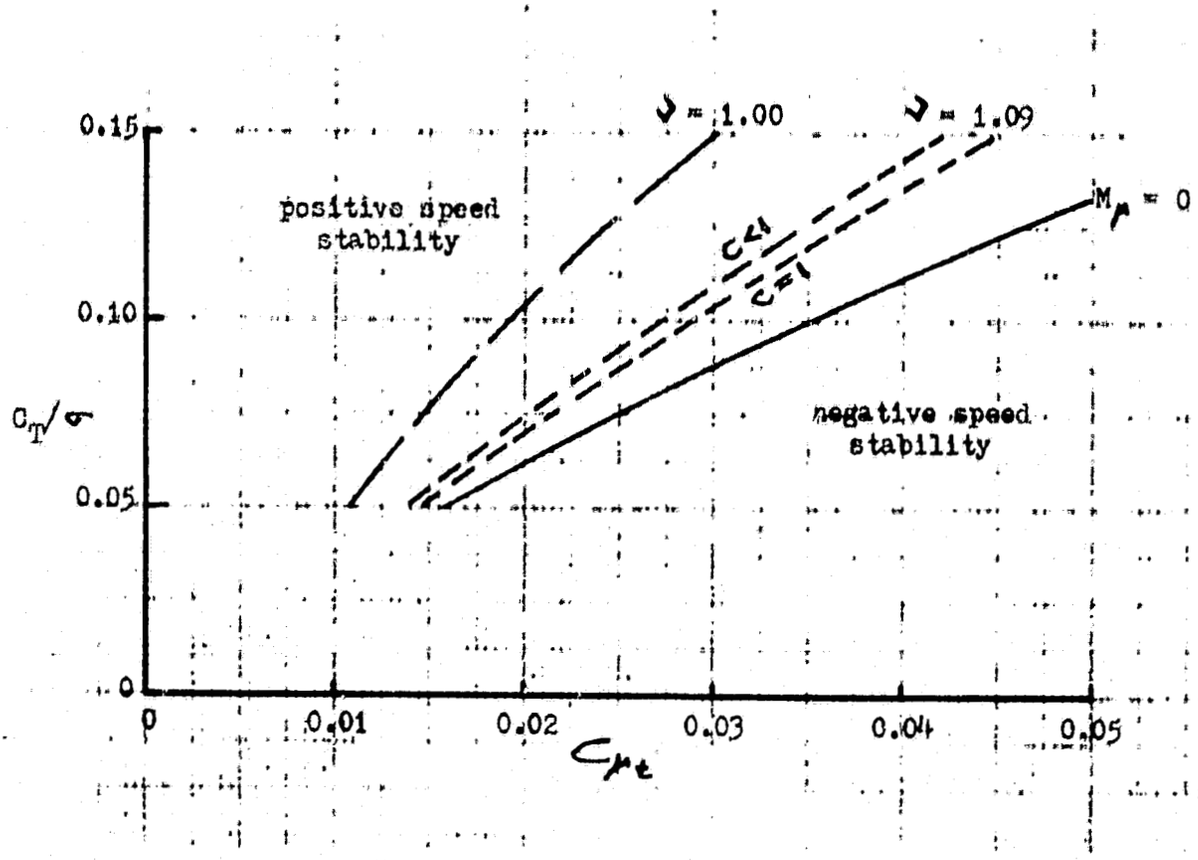

Figure 11 Boundary for zero speed stability, with pitch/flap coupling $K_p = 0.5$ ($\sigma = 0.085$).

1. Report No.	2. Government Accession No.	3. Recipient's Catalog No.
NASA TM-78,443		

4. Title and Subtitle	5. Report Date
CALCULATED HOVERING HELICOPTER FLIGHT DYNAMICS WITH A CIRCULATION CONTROLLED ROTOR	6. Performing Organization Code

7. Author(s)	8. Performing Organization Report No.
Wayne Johnson and Inderjit Chopra*	A-7227
	10. Work Unit No. 505-10-22

9. Performing Organization Name and Address	11. Contract or Grant No.
Ames Research Center, NASA, and Aeromechanics Laboratory, U.S. Army Aviation R&D Command, Ames Research Center, Moffett Field, Calif. 94035	

12. Sponsoring Agency Name and Address	13. Type of Report and Period Covered
National Aeronautics and Space Administration, Washington, D.C. 20546, and U.S. Army Aviation R&D Command, Ames Research Center, Moffett Field, Calif. 94035	Technical Memorandum
	14. Sponsoring Agency Code

15. Supplementary Notes

*NRC Postdoctoral Research Associate, Ames Research Center, NASA.

16. Abstract

The flight dynamics of a hovering helicopter with a circulation controlled rotor are analyzed. The influence of the rotor blowing coefficient on the calculated roots of the longitudinal and lateral motion is examined for a range of values of the rotor lift and the blade flap frequency. The control characteristics of a helicopter with a circulation controlled rotor are discussed. The principal effect of the blowing is a reduction in the rotor speed stability derivative. Above a critical level of blowing coefficient, which depends on the flap frequency and rotor lift, negative speed stability is produced and the dynamic characteristics of the helicopter are radically altered. The handling qualities of a helicopter with negative speed stability are probably unacceptable without a stability augmentation system.

17. Key Words (Suggested by Author(s))	18. Distribution Statement
Circulation controlled rotor Helicopter flight dynamics	Unlimited STAR Category — 01

19. Security Classif. (of this report)	20. Security Classif. (of this page)	21. No. of Pages	22. Price*
Unclassified	Unclassified	39	$4.00

*For sale by the National Technical Information Service, Springfield, Virginia 22161